Published in Marine & Petroleum Geology, Vol. 113, March 2020 doi.org/10.1016/j.marpetgeo.2019.104147

Architecture and paleogeography of the Early Paleozoic carbonate systems in the east-central Tarim Basin (China): constraints from seismic and well data

Yuan Huang [a, *], Tailiang Fan [b], Fabrizio Berra [c]

[a] *SINOPEC* Petroleum Exploration and Production Research Institute, Beijing 100083, China.

[b] School of Energy Resources, China University of Geosciences, Beijing 100083, China.

[c] Università degli Studi di Milano, Dip. Scienze della Terra "A. Desio", Milano, Italy.

[*] Corresponding author. *SINOPEC* Petroleum Exploration and Production Research Institute, Beijing 100083, China. Email address: yhuang621@gmail.com (Yuan Huang)

Abstract

The evolution of the Cambrian-Middle Ordovician carbonate systems in the east-central Tarim Basin, northwestern China, has been investigated using 2D seismic profiles and well data. Interpretation was performed on seismic profiles flattened along an originally horizontal surface (black shale at the base of the Cambrian), to remove the effects of post-depositional deformations. Six seismic facies differently arranged in six seismic stratigraphic units record four major stages of architectural evolution, from ramp to flat-topped systems, with differences from north to south: (1) the onset of a homoclinal ramp over a clayey unit at the beginning of Early Cambrian; (2) the development of a prograding carbonate platform characterized by restricted (evaporitic) facies in the inner platform domain during Early Cambrian to Late Cambrian; (3) the development of a first prograding (to backstepping) and the aggrading (retrograding to the north) platform during Lower Ordovician; (4) the development of a prograding/retrograding to aggrading final platform during Middle Ordovician. The basinward (eastward) progradation of the carbonate platform edge has been reconstructed in time steps, highlighting differences from the north to the south of the study area in terms of amount of progradation, platform-to-basin relief and depositional surfaces, likely controlled by differences in subsidence and environmental factors.

The identification of the four major stages in the evolution of the lower Paleozoic succession of the Tarim Basin was likely controlled by changes in the rate of creation/destruction of accommodation space, due to the interplay between eustatic

changes and tectonic events. The demise of the Cambrian to Middle Ordovician carbonate system is associated with a major tectonic event, recorded by a tilting of the succession toward the east (onlapped by sediments coming from the east) and an the uplift (bulge) of the western part of the study area.

Key words: Tarim Basin; carbonate platforms; Cambrian; Ordovician; paleogeography; sedimentary evolution; seismic interpretation

1. Introduction

Interpretation of subsurface successions may be complex when well data are scarce, as seismic profiles are poorly constrained in terms of attribution of seismic facies to lithological units, facies and depositional environments. In these cases, geometric constraints on the architecture of sedimentary bodies may contribute to improve the seismic profile interpretation. Nevertheless, present-day geometry of seismic reflectors may be deceptive, because it is necessary to understand whether the observed geometry in a seismic profile preserves the original geometry at the time of deposition or if it results from post-depositional deformations. To understand this possible pitfall in seismic interpretation, two elements need to be considered: a) the expected geometry of the considered depositional system (it is therefore necessary to have basic information regarding the type of deposits and their environmental interpretation, typically provided by well data) and b) the identification of the possible evidence that may documents the type and time of, if existing, post-depositional deformation (suggested, for instance, by unrealistic geometry of seismic reflectors in terms of dipping and relationships – such as onlap, downlap, unconformities - with other geological surfaces with seismic expression).

This approach (i.e., looking for geometric constraints and for the evidence of post-depositional deformation in order to reconstruct the geometry of sedimentary bodies at the time of deposition) may be useful also in analyzing already interpreted seismic profiles, possibly contributing to propose alternative interpretations (and, thus, stimulating discussion in the scientific community). With this approach, the re-consideration (taking into account the possible effects of post-depositional deformations on the original architecture of the succession) of some previously interpreted seismic profiles from the Tarim Basin (northwest China) provided alternative interpretations of the stratigraphic architecture of subsurface successions.

The study focuses on attached carbonate platform systems facing basinal

domains, that were widespread in the Tarim Basin from Early Cambrian to Middle Ordovician. These platforms host numerous gas reservoirs (Jia, 1997), a fact that makes the understanding of the evolution of these carbonate systems critical for hydrocarbon exploration. Numerous previous studies about the overall Tarim carbonates focused on the stratigraphy and paleogeography (Zhao et al., 2010; Lin et al., 2011; Zhao et al., 2011; Chen et al., 2015), depositional architectures of platforms and platform evolution (Gao et al., 2006; Fan et al., 2007, 2008; Gu et al., 2009; Wang et al., 2011a; Zhao et al., 2014; Gao and Fan, 2015; Ni et al., 2015; He et al., 2017), the growth mode and characteristics of reef buildups (Xiao et al., 1996; Liu et al., 2003; Gu et al., 2005; Bai et al., 2017a, 2017b) and controlling parameters, including tectonics, subsidence, eustasy, climate/temperature, salinity and nutrients supply (Zhang et al 2014; Zhao et al., 2014; Liu et al., 2016; He et al., 2017; Zhang, 2017).

20 seismic profiles and 13 selected wells were considered to further detail the evolution of the Cambrian and Ordovician carbonate successions in east-central Tarim Basin, in order to reconstruct the evolution of the depositional systems through time and facies distribution, as well as to identify the role of post-depositional tectonics on the present-day geometry recorded in the seismic profiles.

2. Geological setting

2.1 Tectonic setting

The Tarim Basin, located in northwest China, is the largest petroliferous superimposed basin in China with an area of 56 $\times 10^4$ km^2 (Gao and Fan, 2015), with a crystalline basement of Pre-Neoproterozoic age (Jia, 1997; Yu et al., 2016), bounded by the South Tianshan tectonic belt to the north, the Kunlun orogenic belt to the southwest and the Altyn orogenic belt to the southeast (Xiao et al., 1990; Zhang, 1994; Jia, 1997) (Fig. 1A). The present-day orientation of the Tarim Basin results from a clockwise rotation of about 90° with respect to the early Paleozoic orientation. Since the Neoproterozoic, the Tarim Basin was affected by extension due to the break-up of the Rodinia Supercontinent (Xu et al., 2005; Feng et al, 2007; Lin et al., 2011). From Late Neoproterozoic to Early Ordovician, passive continental margins developed, facing the Paleo-Asian Ocean to the west and the Proto-Tethys Ocean, characterized by the presence of several microcontinents detached from Gondwana (Fig. 1B; Wang et al., 2017), to the east. Carbonate platforms developed in the central-western Tarim

Block, when continental rifts developed around Tarim Block producing the Manjiaer depression in the eastern Tarim Block (Zhao et al., 2011; Zhang et al., 2015). Subduction caused the beginning of the collision of the Kunlun and Tianshan blocks with the Tarim Block at the end of Early Ordovician (Zhang et al., 2007; Ye et al., 2008; Neng et al., 2016). Tarim Block underwent convergence since the Middle Ordovician (He et al., 2008), causing the development of paleo-uplifts in southwest, central and northern areas (Fig. 1A) (Wu et al., 2009; He et al., 2015). A foreland basin was formed from Late Ordovician to Middle Devonian (Zhu et al., 2008).

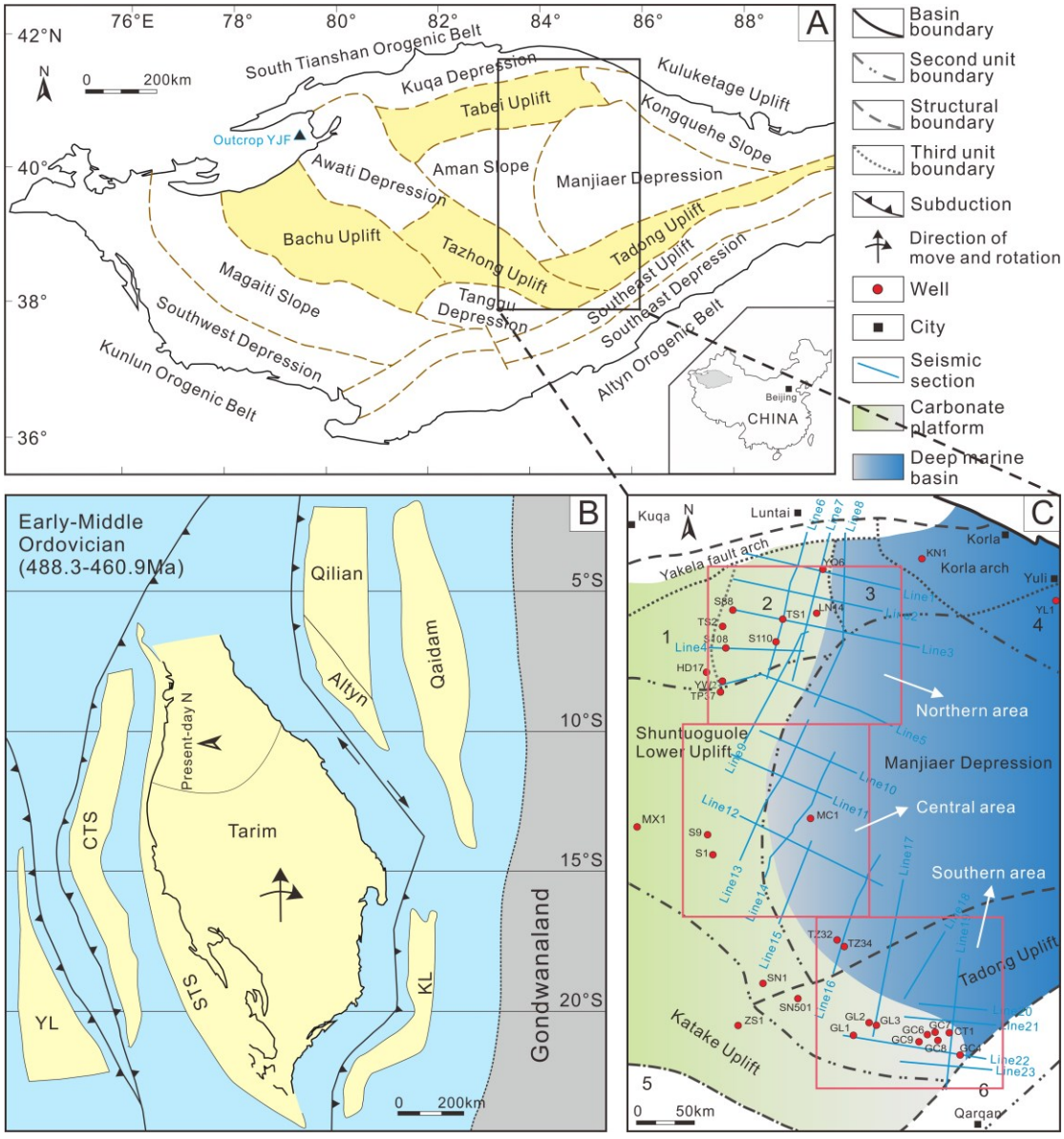

Fig. 1. (A) Sketch of the Tarim Basin showing its subdivision in different units (modified from Lin et al., 2011) and location of study area (black box). **(B)** Paleogeography of the Tarim and adjacent micro-continental blocks in the Ordovician (modified from Torsvik and Voo, 2002; Wang et al., 2017); CTS = Central Tianshan; QL = Qilian; STS = South Tianshan;

KL = Kunlun; YL= Yili. **(C)** General depositional setting of the study area with the position of wells and seismic sections. (1. Halahatang sag; 2. Akekule arch; 3. Caohu sag; 4. Kongquehe slope; 5. Tanggubasi sag; 6. Luobuzhuang arch).

From Cambrian to the end of the Ordovician (Zhang et al., 2015), the carbonate succession of the eastern Tarim Basin was characterized by a shelf domain to the west (Fig. 1C) (where algal limestone/dolostones and grainstones dominate) and by a major depression to the east, where pelagic carbonates are present (Gao and Fan, 2015; Ni et al., 2015). In the inner platform domain, major unconformities (Fig. 2) mark the boundary between Upper Cambrian and Lower Ordovician successions and the top of the Middle Ordovician Yijianfang Formation, covered in northern area by the upper Ordovician succession along a major erosional surface.

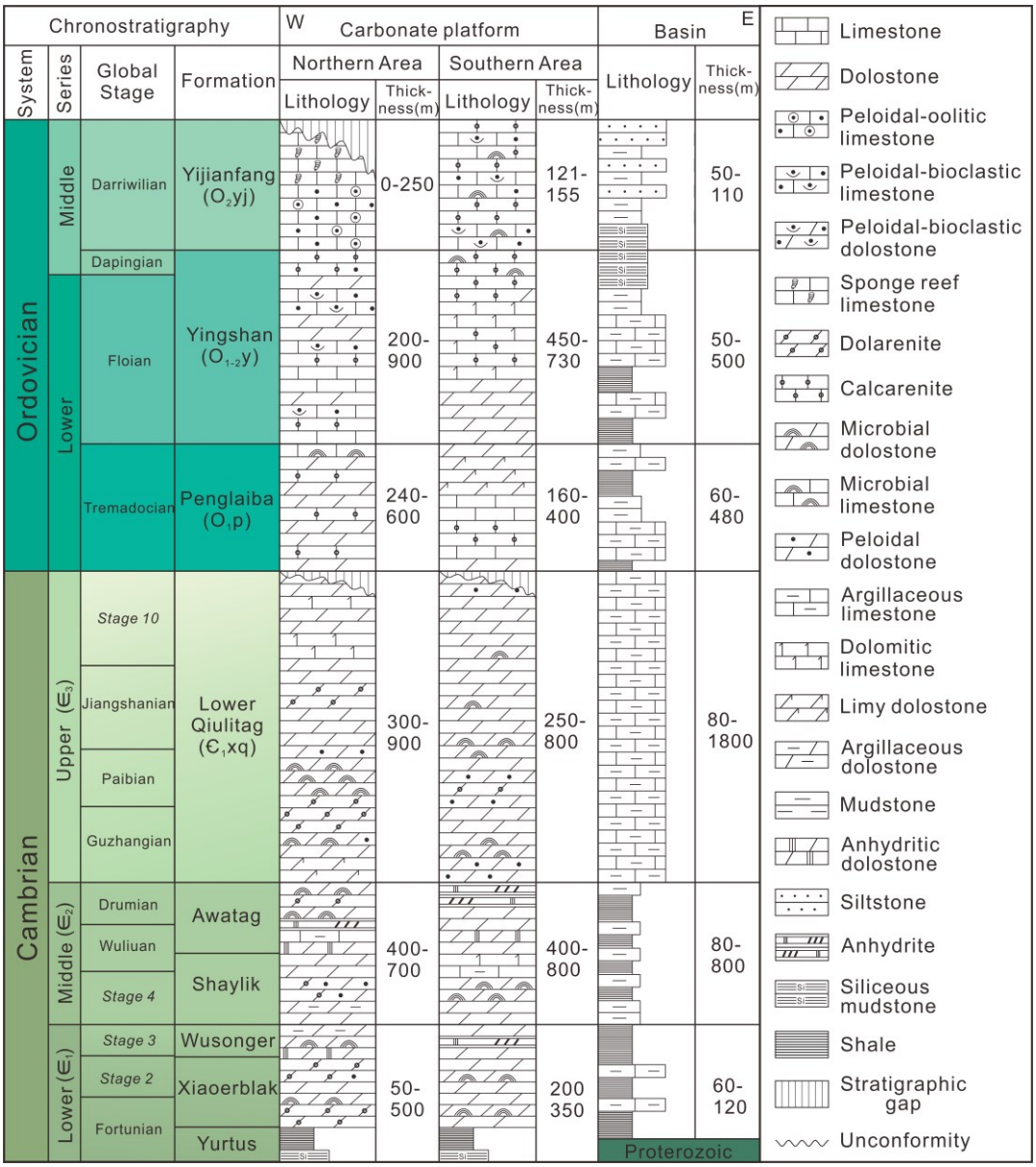

Fig. 2. Stratigraphy of the Cambrian to Middle Ordovician succession in the study area

(modified from Zhu et al., 2016; Fu et al., 2017).

2.2 Facies and architecture of Early Paleozoic carbonate platforms of the Tarim Basin

The Lower Paleozoic succession of the Tarim Basins is characterized by different carbonate systems, each of them documenting the transition from shallow water to basinal settings (Fig. 2). In detail, previous studies identified two major carbonate systems (Gu et al., 2005; Gu et al., 2009; Fan et al., 2007, 2008; Ni et al., 2015; Gao et al., 2012; Chen et al., 2015; Gao and Fan, 2015; He et al., 2017):

a) a carbonate ramp-basin system (Early Cambrian), characterized by a low relief carbonate unit observed in seismic profiles across the Tarim Basin. Seismic facies distribution and geometry (together with core data) suggest an interpretation of this unit as a carbonate ramp (Gao et al., 2006; He et al., 2017) composed of argillaceous dolostones and dolarenites containing algal-clasts;

b) a set of overlying rimmed carbonate platform to basin systems (Middle Cambrian to Middle Ordovician) develops above the Lower Cambrian ramp. The carbonate succession is characterized by a gradual increase of the platform-to-basin relief (Gao and Fan, 2015), leading to overlying rimmed platforms, separated by major reflection surfaces, some of them documenting subaerial exposures observed in wells. The general trend is progradational in the northern area of the study area, whereas progradation is less intense in the southern area, where some retrogradational episodes are also observed.

Further constraints about the facies types and distribution (Liu et al., 2003; Gu et al., 2005; Bai et al., 2017a, 2017b) are provided by outcrops of Cambrian and Ordovician successions (exposed mostly along the western border of the Tarim Basin). The Middle-Upper Cambrian rimmed platform is dominated by algal dolostones interbedded with dolarenites. Microbial buildups and shoals characterize the platform margin (Liu et al., 2016; Bai et al., 2017a). Slope facies of the rimmed platforms in the Early Ordovician consist of laminated dolostones and limestones interbedded with grainstones. In the Middle Ordovician, the platform top lithofacies in the southern area include peloidal-bioclastic limestones and calcarenites intercalated with algal-clasts as well as reef-building fossils (Gu et al., 2005, 2009; Zhang, 2017).

Previous studies describe a general eastward (in present day coordinates)

migration of the shelf margin trajectory from the Early Cambrian to Early Ordovician (Chen et al., 2015). In Middle Ordovician (Zhang et al., 2015; Gao et al., 2016; Jiang et al., 2017), the platforms prograded basinward, with the development of patch reefs in the inner platform and along the shelf margin, from north to south. Differently, Gao and Fan (2015), Yu et al (2016), Neng et al (2016) interpreted the Middle Ordovician platforms in Tabei area and Tazhong area as isolated platforms whose development was controlled by tectonic uplifts.

3. Data and methods

The database used for this study includes of 23 seismic industrial 2D seismic profiles (Sinopec China database; Fig. 1C), 13 selected wells and observations from outcrop analogues (Fig. 1A and 1C). The 2D seismic regional dataset was acquired and processed for hydrocarbon exploration, across an area of ~5.9×10^4 km^2. The studied seismic profiles extend from the platform top to the basinal area of the Cambrian to Middle Ordovician succession. Seismic interpretation was conducted on Move™ (Midland Valley), identifying major seismic unconformities and seismic facies by using standard seismic stratigraphic interpretation techniques (Mitchum et al., 1977). In each seismic unit, seismic facies were characterized according to the reflection features (amplitude, frequency and continuity) and, where possible, referred to lithologies (Fig. 3) from well data according to Liu et al (2016) and Paumard et al (2017).

To better investigate the depositional systems and reconstruct the paleogeography, the present-day geometry of the seismic surfaces has been analysed in order to define possible originally horizontal surfaces that were deformed after deposition. This step is critical, because during interpretation it is necessary to understand if the present-day geometries (such as inclined reflectors) represent the depositional geometry or result from post-depositional deformations. Retrodeformation of the succession is possible after the identification of seismic reflectors interpreted as originally horizontal, according to their geometry, lithology and relationship with underlying and overlying surfaces. The analyses of the 23 seismic images permitted to identify, as reference surface, the base of the Cambrian succession (surface T_9^0, Chen et al., 2007): this surface covers a seismic facies characterized by continuous, parallel high-amplitude reflectors that suggest its original horizontal geometry. Furthermore, this succession consists of black shale (fine-grained sediments, therefore forced to

deposit at a very low-angle or horizontal, not compatible with the present-day dip angle of the seismic reflectors) deposited during global sea level rise (Banerjee et al., 1997; Zhu et al., 2016).

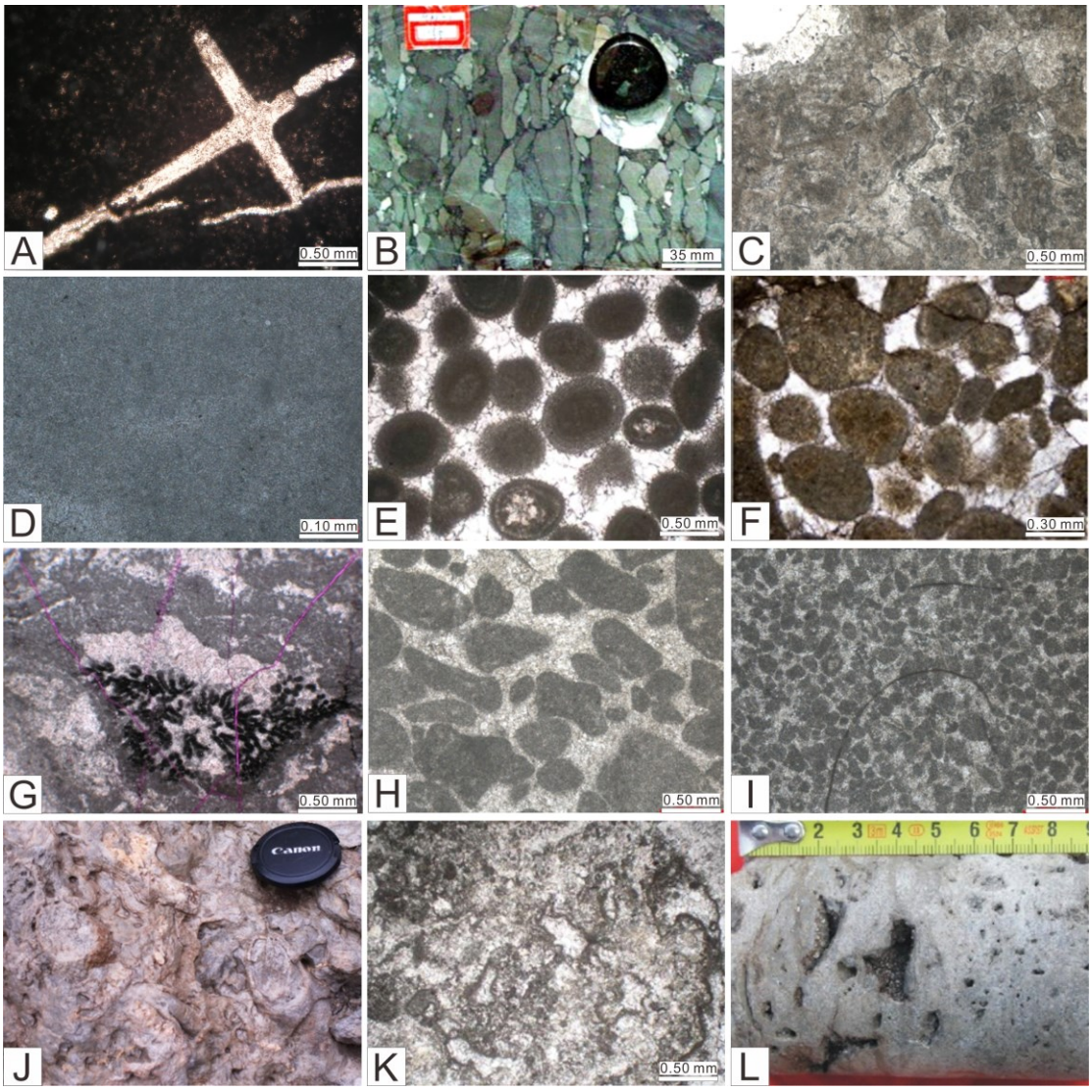

Fig. 3. Cores and outcrops photographs and thin-section photomicrographs showing facies and microfacies of the Cambrian to Ordovician carbonates of Tarim Basin. **(A)** Argillaceous limestones with siliceous spicules, basin; plane-polarized light (PL), well YL1, 4379 m, Lower Cambrian ($\in_1$). **(B)** Graded calcirudites, slope breccias; well KN1, Lower Ordovician. **(C)** Finely-medium crystalline dolostone, inner carbonate platform; PL, well TS1, 6650 m, Lower Ordovician Penglaiba Formation (O_{1p}). **(D)** Micritic limestone, lagoon; PL, well S88, 5535 m, Lower Ordovician Yingshan Formation ($O_{1\text{-}2y}$). **(E)** Well-sorted dolomitized oolitic grainstone, shoal; well TS1, 7710 m, Middle Cambrian. **(F)** Sparry grainstone composed of rounded ooids and intraclasts, shoal; PL, well SN501, Middle Ordovician Yijianfang Formation (O_{2yj}). **(G)** *Epiphyton* in dolomitized mounds with fractures filled by calcite (purple colour, stained with alizarin); PL, well GC4, 5505.4 m (O_{2yj}). **(H)** Rudstone, shoal; PL,

well TS1, 5860 m (O_{1-2y}). **(I)** Doloarenite, shoal; PL, well TS1, 6590 m (O_{1p}). **(J)** Bioclastic limestone with receptaculitids, shoal; Outcrop YJF (O_{2yj}). **(K)** Algal dolostone, microbial reef; PL, well TS1, 8030 m ($\in_1$). **(L)** Finely crystalline dolostone, showing solution vugs; Well TS1, 7874.08 m, Upper Cambrian ($\in_3$).

Seismic facies, their distribution and their physical properties have been interpreted according to the retrodeformed geometry, cross-checking the facies interpretation with, where possible, by well data, validating a stratigraphic architecture that takes into account facies distribution and the extension of exposure/erosional surfaces marking the boundary of diverse carbonate systems, as well as the amplitude of the base-level fluctuations.

4. Seismic facies interpretation and stratigraphic units

4.1 Seismic facies

In the seismic profiles of the carbonate platforms in Tarim Basin, six main seismic facies are recognized on account of their reflection characteristics (internal reflection geometries, amplitude, continuity) and external geometry. Lithological interpretation, constrained by outcrop and well data, were applied to the original geometry at the time of deposition (Fig. 4).

4.1.1 Seismic facies 1 (SF1): parallel to slightly converging, continuous and high amplitude tabular reflectors

Seismic facies SF1 is composed of moderate to high amplitude continuous reflectors, parallel to major seismic reflectors bounding this seismic facies (Fig. 4). This seismic facies, crossed by well YL1, represents argillaceous limestones interbedded with mudstone and laminated clay, indicating pelagic sedimentation in low-energy condition (Fig. 3A) on an almost flat sea-bottom: SF1 is thus interpreted as the seismic expression of a bedded, originally horizontal basinal succession. This seismic facies, observed in the eastern part of the studied seismic profiles, can be followed for tens of kilometers (Fig. 5A and 5D). Toward the west it is possible to recognize a slight divergence of the reflectors. The gradual transition from parallel to slightly converging reflectors in SF1 allows the interpretation of this seismic facies as hemipelagic deposits (parallel reflectors) gradually passing to a basinal fan (slightly converging reflectors). When flattened, both the internal reflectors and the bounding

surfaces are almost horizontal, whereas in the present-day attitude they reach different dips in different seismic profiles.

Seismic facies	Reflection characteristics	Interpretations	Development
SF1 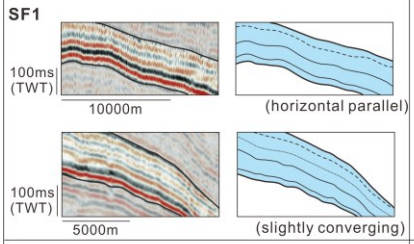	Sub-horizontal to parallel reflections Continuous Moderate to high amplitude	**Basin** **Outer ramp-Basin**	Cambrian and Ordovician Lower Cambrian
SF2 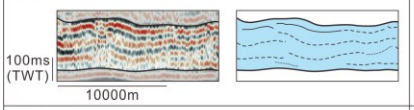	Sub-parallel to parallel reflections Semi-continuous Moderate to high amplitude	**Inner platform** **inner ramp**	Cambrian and Ordovician Lower Cambrian
SF3 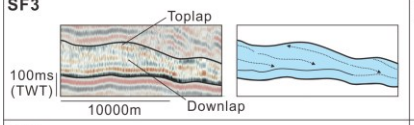	Downlap and toplap reflection terminations Shingled/Oblique parallel clinoforms Semi-continuous Moderate to high amplitude	**Middle ramp**	Lower Cambrian
SF4 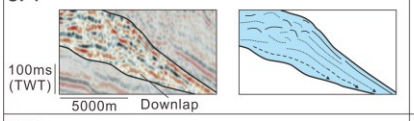	Downlap reflection terminations Complex sigmoid oblique clinoforms Semi-continuous Moderate to high amplitude	**Slope**	Cambrian and Ordovician
SF5 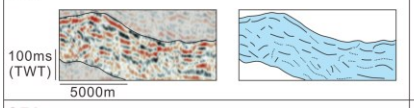	Chaotic to contoured reflections Discontinuous Low to moderate amplitude	**Shoal** (Platform margin/ platform interior)	Cambrian and Ordovician
SF6 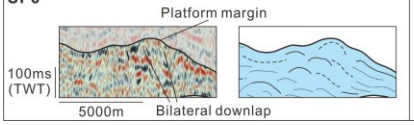	Uneven high-reflective boundaries Bilateral downlap reflection terminations Mound-shaped and chaotic reflections Discontinuous to semi-continuous Low to moderate amplitude	**Reef** (Platform margin)	Cambrian and Ordovician

Fig. 4. Types of seismic facies identified on the 2D seismic data, lithological and depositional interpretation and age distribution.

4.1.2 Seismic facies 2 (SF2): sub-parallel, semi-continuous and moderate-high amplitude reflectors

Seismic facies 2 consists of sub-parallel tabular to swelled reflectors with semi-continuity and moderate to high amplitude (Fig. 4). The external form of the facies displays parallel sheets or sheets drape, with thickness ranging from 50 to 270 ms TWT. This seismic facies is crossed by wells S88 and TS1, where it consists of micritic limestone and fine-medium crystalline dolostones (Fig. 3C and 3D).

Lithological constraints from well data and the characteristics of SF2 support an interpretation as inner platform carbonate deposits characterized by steady and low to medium-energy water condition. In the basal carbonate system (Early Cambrian), SF2 may correspond to inner ramp deposits, whereas in younger systems (middle-upper Cambrian and Ordovician units) SF2 is interpreted as inner platform deposits

(including lagoon or open platform facies).

4.1.3 Seismic facies 3 (SF3) and 4 (SF4): semi-continuous and moderate amplitude clinoforms

Seismic facies 3 and 4 are composed of semi-continuous to discontinuous reflectors with moderate to high amplitude. SF3 and SF4 are characterized by reflectors which have an angular relationship with the underlying seismic facies along a high-rank surface. When flattened, internal reflectors appear as clinoforms, with downlap and toplap reflection terminations (Fig. 4). The clinostratification in SF4 is also documented by the upper bounding reflector that commonly converges with the reflector at the base of these seismic facies. These seismic facies have a lateral extension of 7 to 18 km on average and thickness up to 150 ms TWT (Fig. 5-9, Early Cambrian) and 4-20 km width and up to 400 ms TWT thickness (Middle Cambrian to Ordovician). According to the changes in thickness of these facies, they are interpreted as slopes of low-relief platforms (Early Cambrian, interpreted as grain-supported middle ramp sediments; Fan et al., 2007) or slopes (possibly breccias) of high relief carbonate platforms. This interpretation is supported by data from well KN1 (Fig. 3B).

4.1.4 Seismic facies 5 (SF5): discontinuous reflectors

Seismic facies 5 is characterized by low continuity and low to moderate amplitude reflectors (Fig. 4). SF5 generally comprises discontinuous, irregular reflectors, commonly laterally bordered by Seismic facies 6. SF5 has variable thickness with lateral extension of 2- 20 km (Fig. 5 - 9). Core data from well TS1 reveal that this facies mostly consists of grain-supported bioclastic (mostly algae) debris (Fig. 3E). Composition and geometry suggest its interpretation as back reef, high energy carbonate deposits. Well data of well SN501 from inner platform settings indicate the presence of oolitic and intraclastic limestone (Fig. 3F), bioclastic limestones/dolostones and rudstone/calcarenites/dolarenites (Fig. 3H and 3I), interpreted as shoal facies.

4.1.5 Seismic facies 6 (SF6): homogeneous to poorly continuous reflectors

Seismic facies 6 is characterized by mound-shaped low continuity and low to moderate amplitude reflectors. SF6 has generally a relief and is narrower (1-2.5 km) with respect to the nearby seismic facies and typically characterizes the transition

from parallel to converging high-rank reflectors (Fig. 4). This facies is commonly characterized by bilateral downlap reflection terminations and in some cases displays uneven and truncated high-reflective top boundaries. Well TS1 crossing this seismic facies and outcrop observations reveal the presence of algae-dominated microbial limestones/dolostones (Cambrian and Early Ordovician, Fig. 3K; Bai et al., 2017a, 2017b) and receptaculitids or calathium (Middle Ordovician, Fig. 3J; Gu et al., 2009), indicating high-energy condition. We interpret this seismic facies as reef facies.

4.2 Seismic stratigraphic units and depositional systems

Previous studies defined unconformities and correlative conformities bounding different stratigraphic units in Cambrian and Ordovician: this interpretation rely upon well data, outcrop and seismic data (Yu et al., 2001; Zhao et al., 2010; Gao and Fan., 2015; Liu et al., 2016). The stratigraphic surfaces identified in this study confirm the subdivisions proposed by Tang et al (1997), Zhou et al (2006) and Lin et al (2011) who recognize seven stratigraphic surfaces (T_9^0, T_8^0, T_7^8, T_7^4, associated with subaerial exposures; Liu et al., 2010; Zhao et al., 2010; Chen et al., 2016, and T_8^1, T_8^3, T_7^5) encompassing six carbonate units, each characterized by diverse seismic facies arrangements. The bounding surfaces (Figs. 5 to 9) reflect events that controlled the major changes in the stratigraphic architecture. The six Cambrian and Ordovician units (different for seismic facies association, thickness, relative slope angles, type of bounding surfaces, stratal terminations and stacking patterns) also record differences in the three areal domains: northern (Lunshen area, Fig. 5; Yangwu area, Fig. 6), central (eastern Shuntuoguole area, Fig. 7) and southern domain (northern Gulong area, Fig. 8; Gucheng area, Fig. 9). For each of these six carbonate units, a detailed evaluation of the geometry of the seismic surfaces and facies has been performed, in terms of: i) relationships with underlying and overlying reflectors; ii) present day geometry with respect to the possible geometry at the time of deposition (i.e.; after flattening) and iii) validation of the facies interpretation coherently with the geometry of the internal reflectors.

4.2.1 Early Cambrian depositional system (DS1)

The Early Cambrian depositional system was deposited above an originally almost planar surface T_9^0 capped at the top by a transitional lithofacies boundary (surface T_8^3 Chen et al., 2007; Zhao et al., 2010). This unit thins out from the west to east. The maximum thickness reaches 360 ms (TWT) in the north (Fig. 5 and Fig. 6)

and 190 ms (TWT) in the south (Fig. 8 and Fig. 9). DS1 can be subdivided into three parts. The lowest part shows high-amplitude, parallel, continuous reflectors (seismic facies SF1; Fig. 4). The middle part mainly consists of subparallel to parallel continuous reflectors with high amplitude gradually converting toward the east (seismic facies SF1 to SF3; Fig. 5B). Inclined reflectors (clearly identifiable on the seismic profile flattened along the surface T_9^0) develop between SF1 and SF2 and are interpreted as middle ramp facies (Fig. 5B and Fig. 5D). The upper part of DS1 shows, from west to the east, subparallel low-moderate amplitude and semi-continuous inner platform facies (SF2) evolving to convex-up discontinuous reflectors (SF5-SF6) and moderate amplitude semi-continuous prograding reflection (SF4; Figs. 5B to 9B), interpreted as basinward downlapping beds. The topmost part is characterized by discontinuous mound-shaped reflections with low-amplitude (SF6), bilaterally downlapping to underlying high-amplitude and continuous reflection (Figs. 5 to 9). In the northern area, prograding oblique clinoforms dominate this upper part of DS1 (Fig. 5 and Fig. 6), whereas, in the southern area aggradation is clearly observed (Fig. 9).

4.2.2 Middle Cambrian depositional system (DS2)

System DS2, bounded as its top by seismic unconformity T_8^1, is characterized by a thinning from 100-200 ms TWT on the west to less than 100 ms TWT to the east along a narrow belt characterized by clinostratified reflectors that document a progradation of 5 to 10 km. The prograding belt is characterized by convex up irregular reflectors, interpreted as a platform margin, covered by parallel, overlying reflectors in DS3 (Figs. 5 to 9). The platform margin in the northern area is bounded by a gentle slope displaying complex-oblique clinoforms with toplap terminations (Fig. 5 and Fig. 6), whereas, the margin in the southern area passes to a relative steep slope showing oblique-parallel reflector packages (Fig. 9). The depositional system DS2 is characterized by a gradual increase of the platform-to-basin relief, continuing the evolution observed in the upper part of DS1.

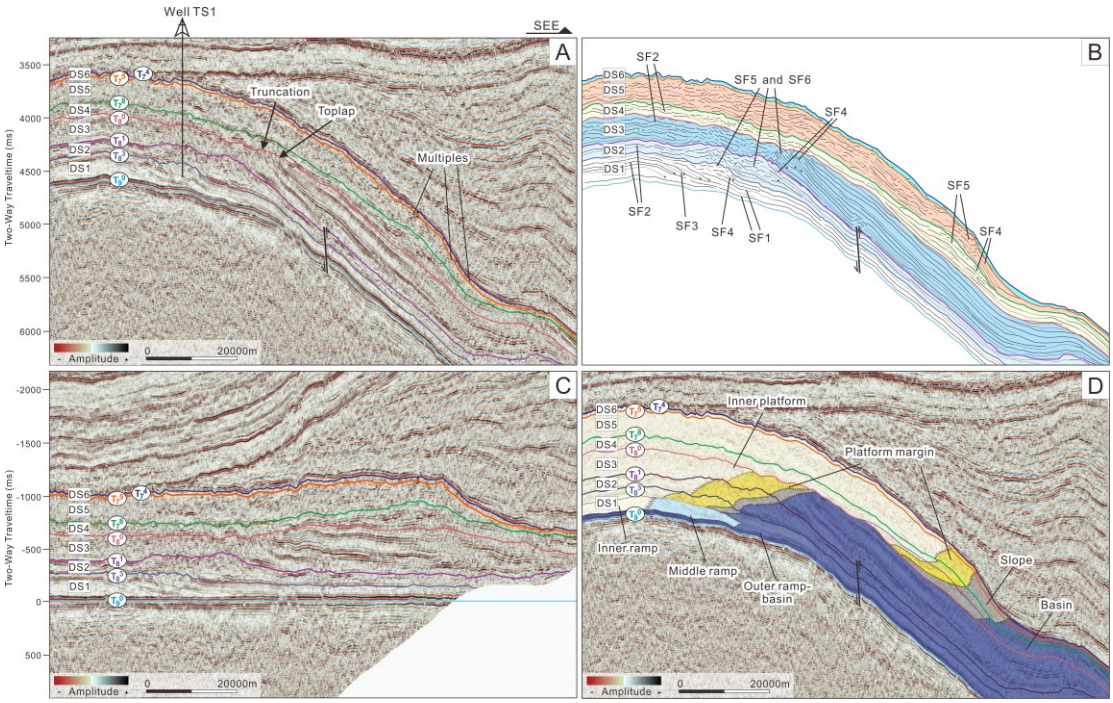

Fig. 5. Un-interpreted (A), flattened (C) and interpreted (B, D) seismic profiles of Line 3 in northern area (see location on Fig. 1C).

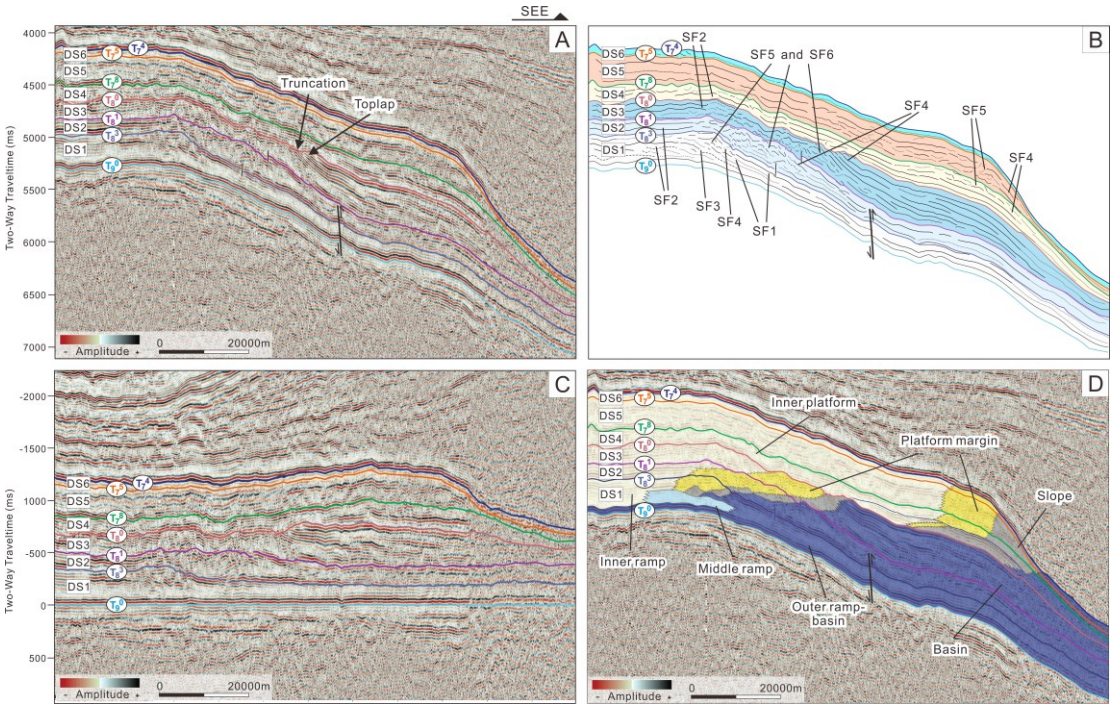

Fig. 6. Un-interpreted (A), flattened (C) and interpreted (B, D) seismic profiles of Line 5 in northern area (see location on Fig. 1C).

4.2.3 Late Cambrian depositional system (DS3)

System DS3, Late Cambrian in age, is bounded by surfaces T_8^1 and T_8^0. T_8^1 represents a change in lithology associated with local erosion (Lin et al., 2011). DS3 in the northern area is approximately 200 ms TWT thick in the platform area (east)

and reaches a thickness of more than 400ms TWT in the western basin (Fig. 5 and Fig. 6), resulting in a gradual reduction of the platform-to-basin relief. The platform margin, dominated by mound-shaped reflectors, is bounded by a slope with a dip angle decreasing with time. The toplap geometry of the slope facies (consisting of parallel-tangential oblique clinoforms, prograding basinward for about 20 km; fig. 6D) suggests a period of reduced creation of accommodation space. In the southern area, DS3 is about 170 ms TWT thick in the east and 70-200 ms in the west (Fig. 8 and Fig. 9), reflecting a reduced sedimentary input in the basin and thus, a gradual increase in the platform-to-basin relief. The platform margin is characterized by convex-up (mound-shape) reflections prograding for 8 to 15 km, with low-angle semi-continuous oblique-parallel clinoforms on the slope. Between north and southern area, an intermediate situation is observed (Fig. 7), with 15-20 km of progradation, a seismic thickness similar to that of the northern area and internal architecture comparable with that of the southern area. The topmost surface of DS3 (T_8^0) is a subaerial erosional surface (Fig. 5 and Fig. 6; Lin et al., 2012), as documented by karst features observed in cores (Fig. 3L) and outcrop.

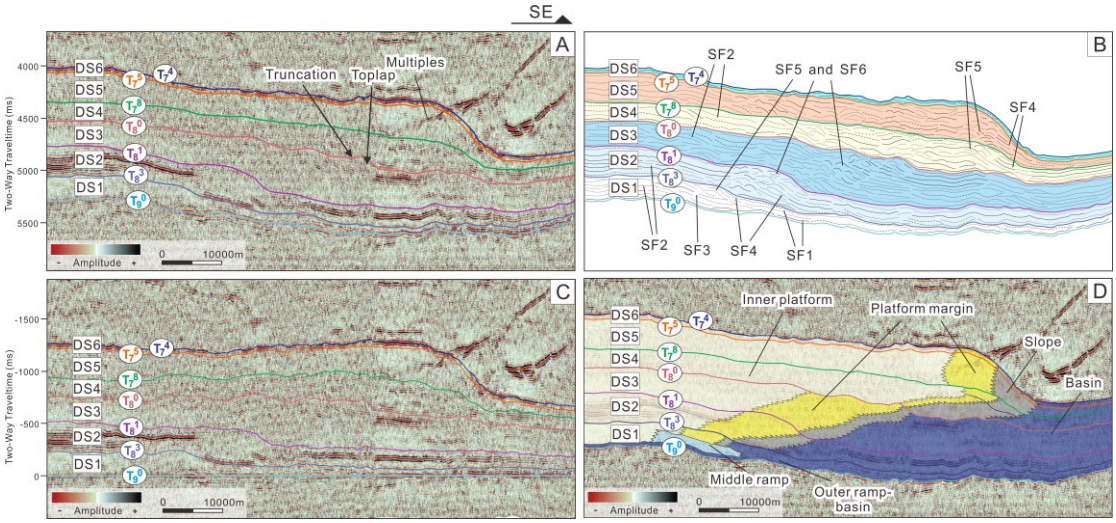

Fig. 7. Un-interpreted (A), flattened (C) and interpreted (B, D) seismic profiles of Line 12 in central area (see location on Fig. 1C).

4.2.4 Early Ordovician (Penglaiba Formation) depositional system (DS4)

Seismic facies and geometry define a platform domain in the west and basinal setting to the east for the System DS4 (Penglaiba Formation, Early Ordovician). The platform-to-basin transition is represented by lens-shaped clinoforms with sigmoid and tangential-oblique patterns (Figs. 5D to 9D). Well data (Gucheng area) document the presence of tight micritic limestone in lower part of Penglaiba Formation (Liu et al., 2017). The upper part of DS4 is dominated by discontinuous low-amplitude

irregular and shingled/hummocky clinoform reflectors (Fig. 4). System DS4 displays, in the retrodeformed seismic profile, variable thickness from basin (100 ms TWT in northern area, Fig. 5C; 90 ms TWT in central area, Fig. 7C; 60 ms TWT in southern area, Fig. 9C) to platform margin (200 ms TWT in northern area, Fig. 5C; 400 ms TWT in central area, Fig. 7C; 300-470 ms TWT in southern area, Fig. 8C and 9C), documenting a new increase of the platform-to-basin relief with respect of the previous system, changing from north to south. The southern area displays steeper slopes and an aggradation trend, whereas the northern and central areas, characterized by progradational and aggradational reflectors, present a large, low-angle slope. Comparing the architecture of DS4 with the underlying DS3, it is possible to recognize, in the northern area, a progradation of about 40 km. DS4 is capped by an erosional truncation (T_7^8; Figs. 5A to 9A), which represents the seismic expression of karst features observed in outcrop (Gao et al., 2016).

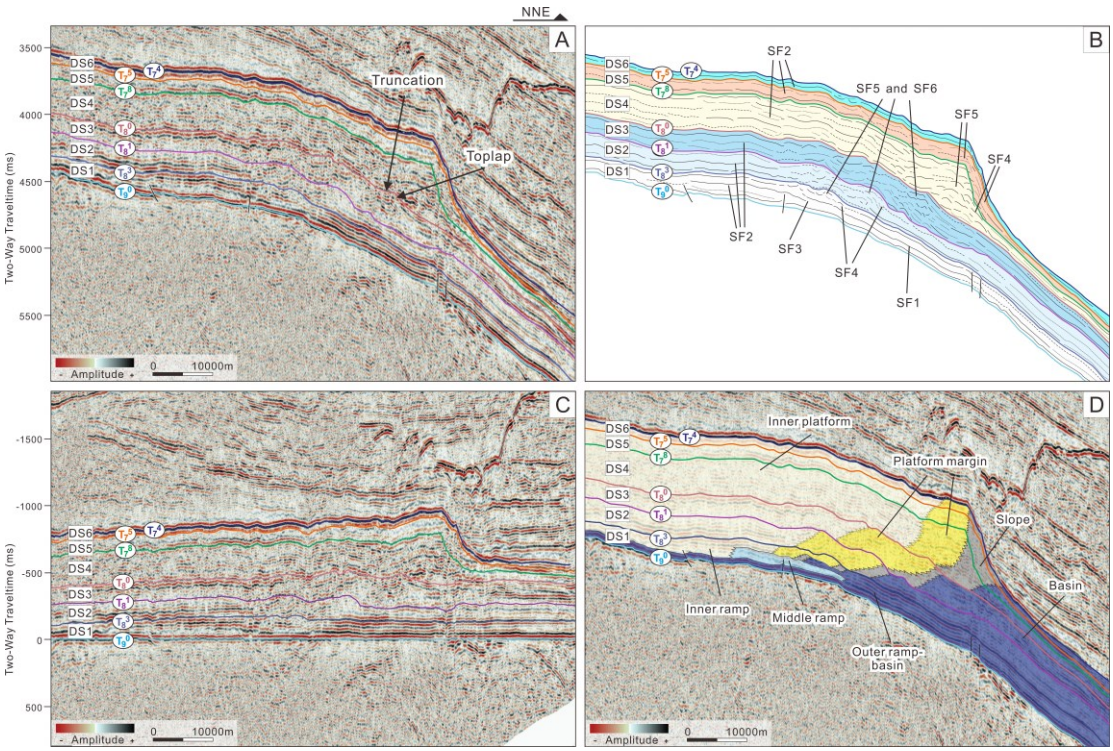

Fig. 8. Un-interpreted (A), flattened (C) and interpreted (B, D) seismic profiles of Line 17 in southern area (see location on Fig. 1C).

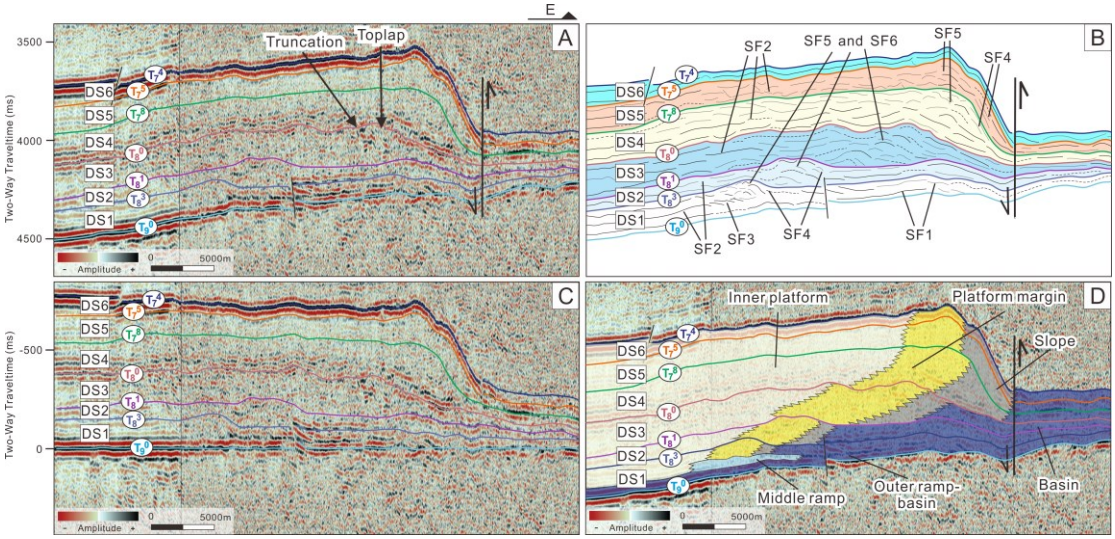

Fig. 9. Un-interpreted (A), flattened (C) and interpreted (B, D) seismic profiles of Line 20 in southern area (see location on Fig. 1C).

4.2.5 Early-Middle Ordovician (Yingshan Formation) depositional system (DS5)

Above unconformity T_7^8, sequence DS5 (Yingshan Formation, Early-Middle Ordovician) displays a roughly constant thickness of about 50 ms TWT in the basinal area (east) and a thickness, in the platform domain, of about 250 ms TWT in the northern area, 330 ms TWT in the central area and 150 ms TWT in the southern area (Figs. 5D to 9D). The eastward-dipping seismic reflectors of this depositional system are crossed by sub-horizontal signals that are interpreted as multiples of overlying, strong reflectors, complicating the seismic interpretation of this depositional system. In the western part of the seismic profiles, sub-parallel, semi-continuous moderate to high amplitude reflections (SF2) are interpreted as platform interior facies. Semi-continuous low-amplitude irregular reflections (SF4) downlapping the underlying unconformity T_7^8 are interpreted as slope facies, that can be identified in most of the seismic sections (Figs. 5B to 9B). These slope facies, characterized by gentle slopes in the northern and central area, border margins with different architecture: backstepping to aggrading in the lower part and forestepping to aggrading in the upper part (Figs. 5 to 7). Slope angle of DS5 appears steeper in the southern area, where the margin displays a prograding to aggrading pattern in the lower part and backstepping to aggrading in the upper part (Fig. 8 and Fig. 9). The upper boundary of DS5 (T_7^5) is an erosional unconformity (Gao et al., 2006; Liu et al 2016).

4.2.6 Middle Ordovician (Yijianfang Formation) depositional system (DS6)

DS6 (characterized by homogenous thickness of 50-60 ms, TWT) is defined at

the base by the erosional surface T_7^5 and at the top by T_7^4 (Lin et al., 2012). The reduced thickness prevents a detailed identification of the seismic facies within this unit. DS6 displays parallel continuous high-amplitude reflections; some local, small, convex-up reflectors have been identified in the inner platform, probably marking the transition to the margin (Figs. 5 to 9). This depositional system marks the end of the Cambrian to Middle Ordovician carbonate platform systems (Fig. 5D and Fig. 9D). Platform top is characterized by exposure and erosion with karst features. The topmost surface (T_7^4) is an onlap surface, with a gradual deposition of younger sediments from east to west (Figs. 5A to 9A). The onlapping succession is characterized by eastward diverging reflectors, supporting the existence of a tilting/folding event after the deposition of the Cambrian-Ordovician carbonate systems (Fig. 5C) and during the deposition of the units onlapping T_7^4, suggesting that deformation affected the onlap surface after its deposition (i.e.; it is not an original depositional surface).

5. Discussion

An alternative stratigraphic interpretation of the Cambrian-Ordovician succession of the Tarim Basin is proposed, considering that the black shale at the base of the succession were deposited horizontally and that no major deformation occurred in the considered time interval, as deduced from the distribution of the identified seismic facies. The 2D seismic profiles have been retrodeformed removing, by flattening the base of the carbonate succession (surface T_9^0, Chen et al., 2007), the post-depositional deformations, allowing the reconstruction of the depositional architecture at the time of deposition. The resulting interpretation differs from previous ones proposed for the same succession (Gao et al., 2006; Gao and Fan, 2015; Ni et al., 2015), for example regarding the position of the platform edge, which in this interpretation is moved basinward with respect to the previous ones. Furthermore, this interpretation suggests a major tectonic deformation at the end of the Ordovician, when an eastward tilting of the succession occurred. This tilting was likely associated with the development of a bulge (partly eroded) in the western part of the seismic lines, with the deposition of a gradually onlapping sedimentary wedge from the east (Fig. 10). This architecture shows strong similarities with a load-induced subsidence in the east, responsible for the development of a distal bulge, uplifting the inner platform domain, where part of the youngest carbonate system has been eroded. The architecture of the resulting basin strongly resembles that of a peripheral foreland basin, likely related to an

orogenic event east of the present-day Tarim Block. After this event, the seismic profiles document a return to a deposition of almost horizontal units.

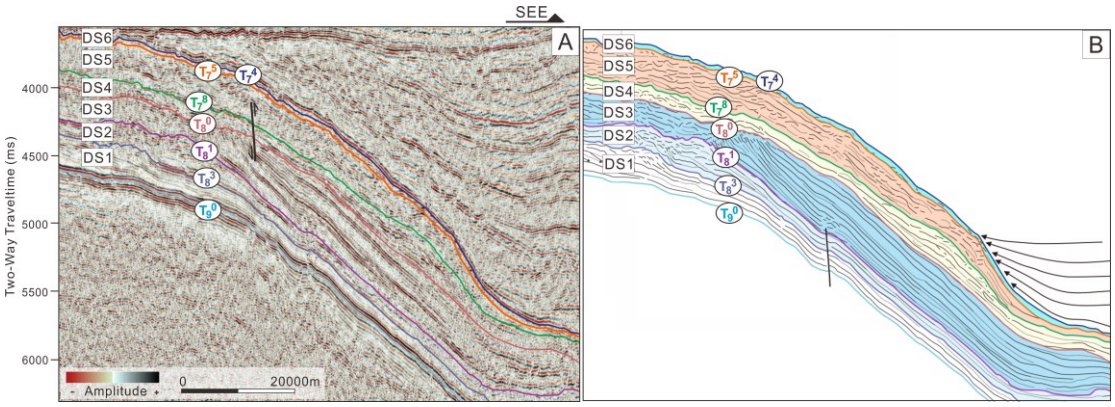

Fig. 10. (A) Uninterpreted flattened seismic section of Line 3 and (B) interpreted section (see location on Fig.1C).

5.1 Paleogeographic evolution

The reconstruction of the different facies belts interpreted in the seismic profiles for each of the depositional systems provided evidence for the changes in the facies distribution, both across time (from Cambrian to Ordovician) and across space, from north to south, of the studied part of the Tarim Basin.

The seismic interpretation of the depositional architecture of the Early Paleozoic carbonate depositional systems suggests a general eastward shift of the platform-slope break (Chen et al., 2015), whose position documents the trajectory of the platform edge (ramp in the earliest stage) from Early Cambrian to Middle Ordovician (Fig. 11).

The entity of progradation from the DS1 (Early Cambrian) to DS3 (Late Cambrian) is approximately 20-30 km in the northern area and 10-16 km in the southern area. From DS3 to DS4 (Early Ordovician), the carbonate platform in the northern area progrades eastward for up to 40 km, whereas in the southern area progradation is reduced to about 5 km. During DS4 to lower DS5 (Early to Middle Ordovician), platform-slope break record retrogradation in the northern area and short-distance eastward progradation in the southern area. From upper DS5 to DS6 (Middle Ordovician), the carbonate platform in the norther area progrades eastward and platform in southern area retrogrades toward inner platform for short distance. The difference in the entity of the progradation in the northern and southern areas may be controlled by the different platform-to-basin relief, higher in the southern area with respect to the northern one and/or by different prevailing directions of currents and wind.

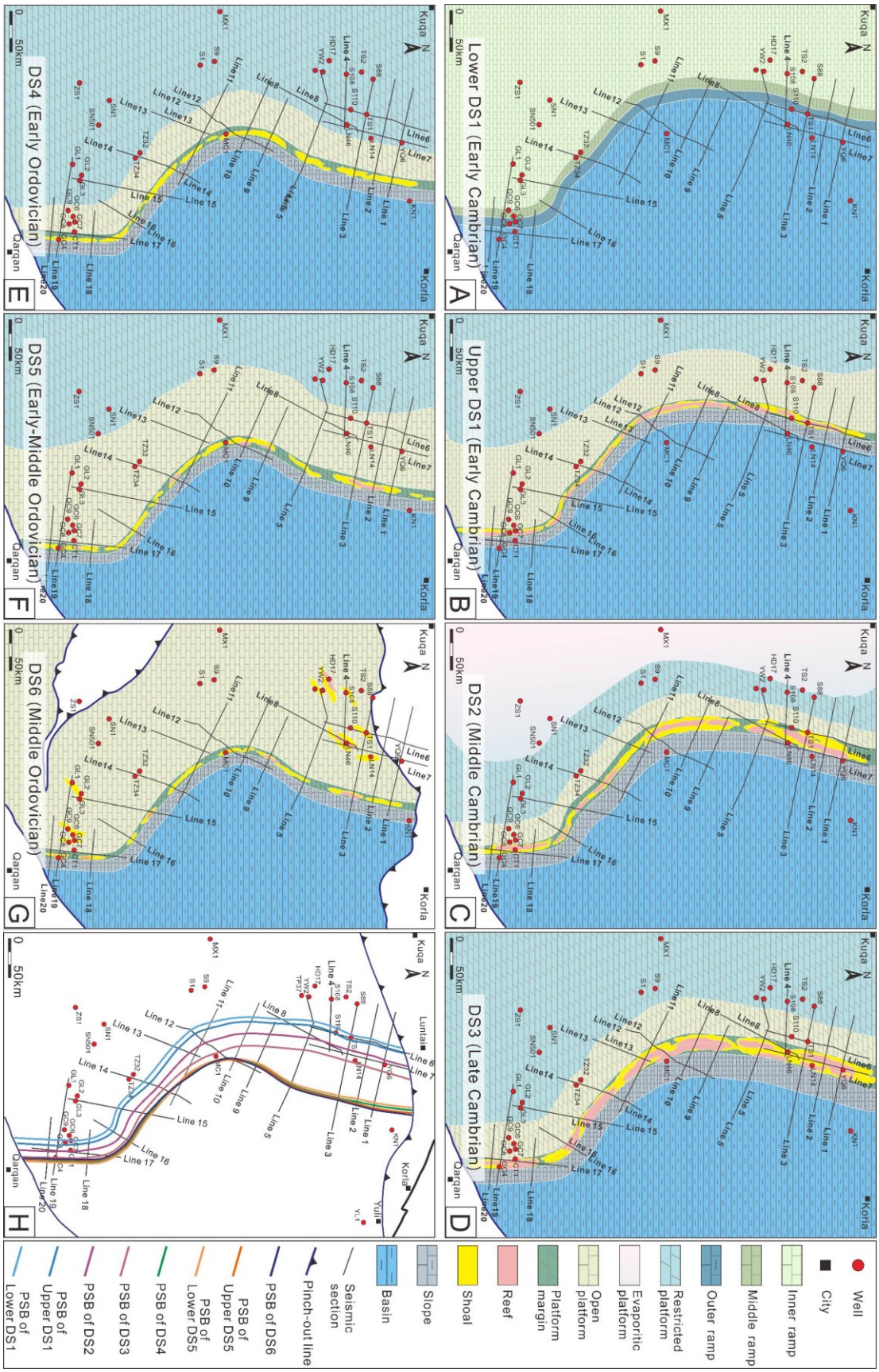

Fig. 11 Traces of the platform-slope breaks (PSB) at different moments of the carbonate system evolution (A to G), showing the general eastward progradation of the carbonate

platforms from Cambrian to Ordovician and synthetic sketch (H) of all the traces of the platform-slope breaks (PSB) at the different moments of the carbonate system evolution, showing the general eastward progradation of the carbonate platforms from Cambrian to Ordovician on a single map.

Seismic interpretations and depositional features (from well data and previous studies) document a different evolution in the northern and southern areas (with transitional features in the central area). Four major stages of carbonate-platform growth (Fig. 12), consistent with paleogeographic evolution (Fig. 13 and Fig. 14), have been recognized.

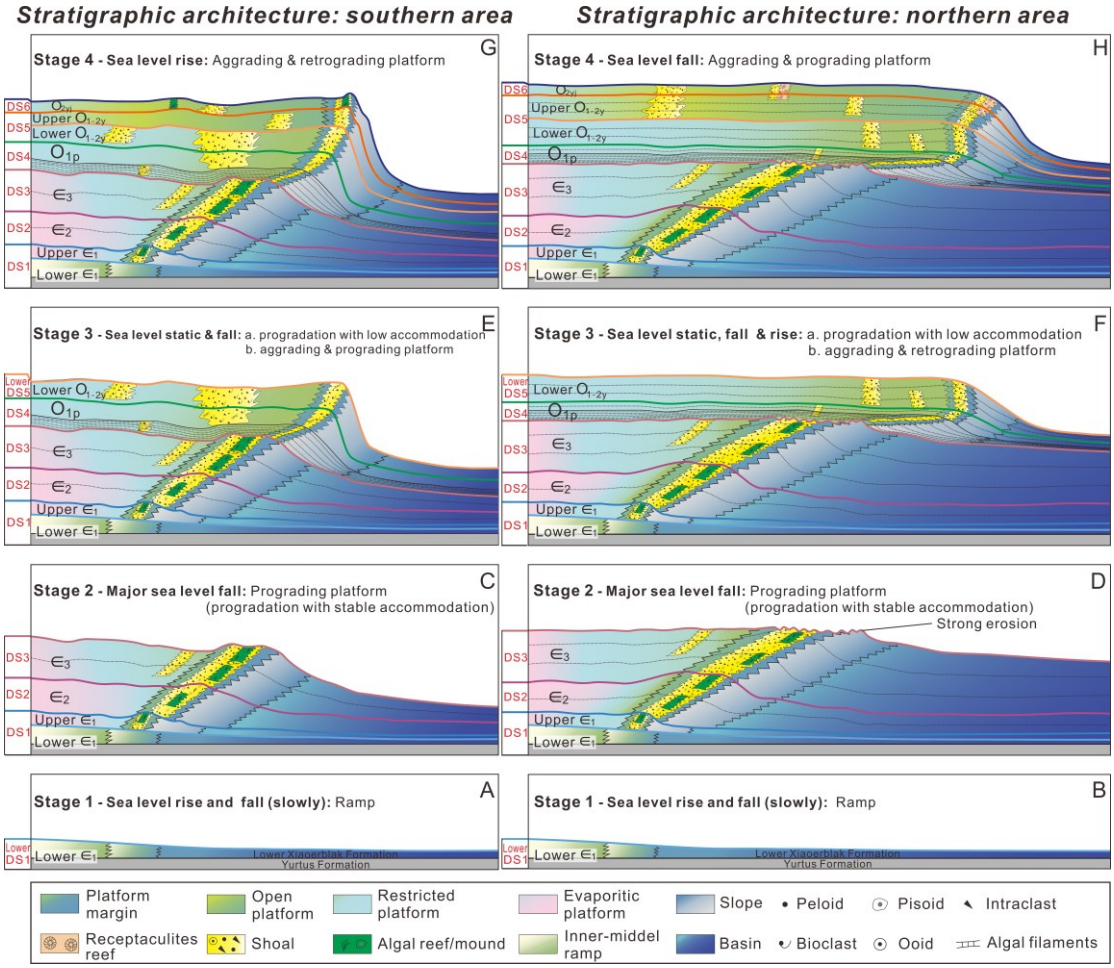

Fig. 12. Schematic evolution of the carbonate ramp/platforms during the Early Cambrian to Middle Ordovician in the northern and southern areas.

Stage 1 (lower DS1):

The deposits of this stage (Yurtus Formation; Fig. 12A and Fig. 12B) cover parallel high-amplitude reflections (Figs. 5 to 9) that are interpreted as black shale deposited originally horizontally during a global sea level rise (Banerjee et al., 1997; Zhu et al., 2016). During the middle part of this stage (lower Xiaoerblak Formation), seismic facies interpretation suggests the development of a uniform, gently inclined

ramp thinning basinward (Fig. 5D, 6D, 7D, 8D and 9D). Subsurface well data are poor to characterize the seismic facies, but coeval outcrops and cores data west of the study area document the presence of dolarenites interbedded with algal dolostones, indicating inner and middle ramp environment (Zhao et al., 2011; Bai et al., 2017a), corresponding in the seismic profile to SF3 (Fig. 4). In Stage 1 the evolution and architecture in the northern and southern area are very similar (Fig. 11D and Fig. 11H), uniformly displaying a middle ramp belt about 10 km wide (Fig. 13A).

Stage 2 (upper DS1 to DS3):

During this stage, the carbonates ramp system evolves to a flat-topped platform that will persist until the middle Ordovician. This architectural evolution may be related to a change in the carbonate-producing biota, as suggested by the appearance of abundant calcareous algae the in marginal area (well TS1, YQ6 and CT1). Previous studies (Chen et al., 2015; Ni et al., 2015; He et al., 2017) documented the presence of evaporite (gypsum and halite) in platform-interior from the topmost Early Cambrian to Middle Cambrian. Fine-medium crystalline dolostones recording traces of dissolved halite crystal observed in well TS1 (also in the Upper Cambrian; Fig. 3I) document deposition in an evaporitic-restricted inner platform (Fig. 12C, 12Dand 13B). This restricted, flat-topped platform is bounded eastward by a rim where microbial buildups associated with shoal deposits (Fig. 13B) are present. Core data from wells (TS1 and CT1) crossing these buildups as well as outcrop data (Bai et al., 2017b) show dolomitized grainstone or boundstone dominated mainly calcareous algae (including *Nephrocytium*, *Girvanella* and *Epiphyton*), representing the reef facies. The entire stage is characterized by a progradational trend from the upper S1 to S3 (Fig. 12C and 12D). Progradation is stronger and the succession is thicker in the northern area, suggesting different environmental and tectonic conditions (higher sediment supply and subsidence, different transport coefficient; Williams et al., 2011). The end of this stage (top of DS3) is marked by a truncated toplap surface (Figs. 5A to 9A), that records the exposure and erosion of platform due to a relative sea level fall. Erosion is strongest in the northern area (Fig. 12D).

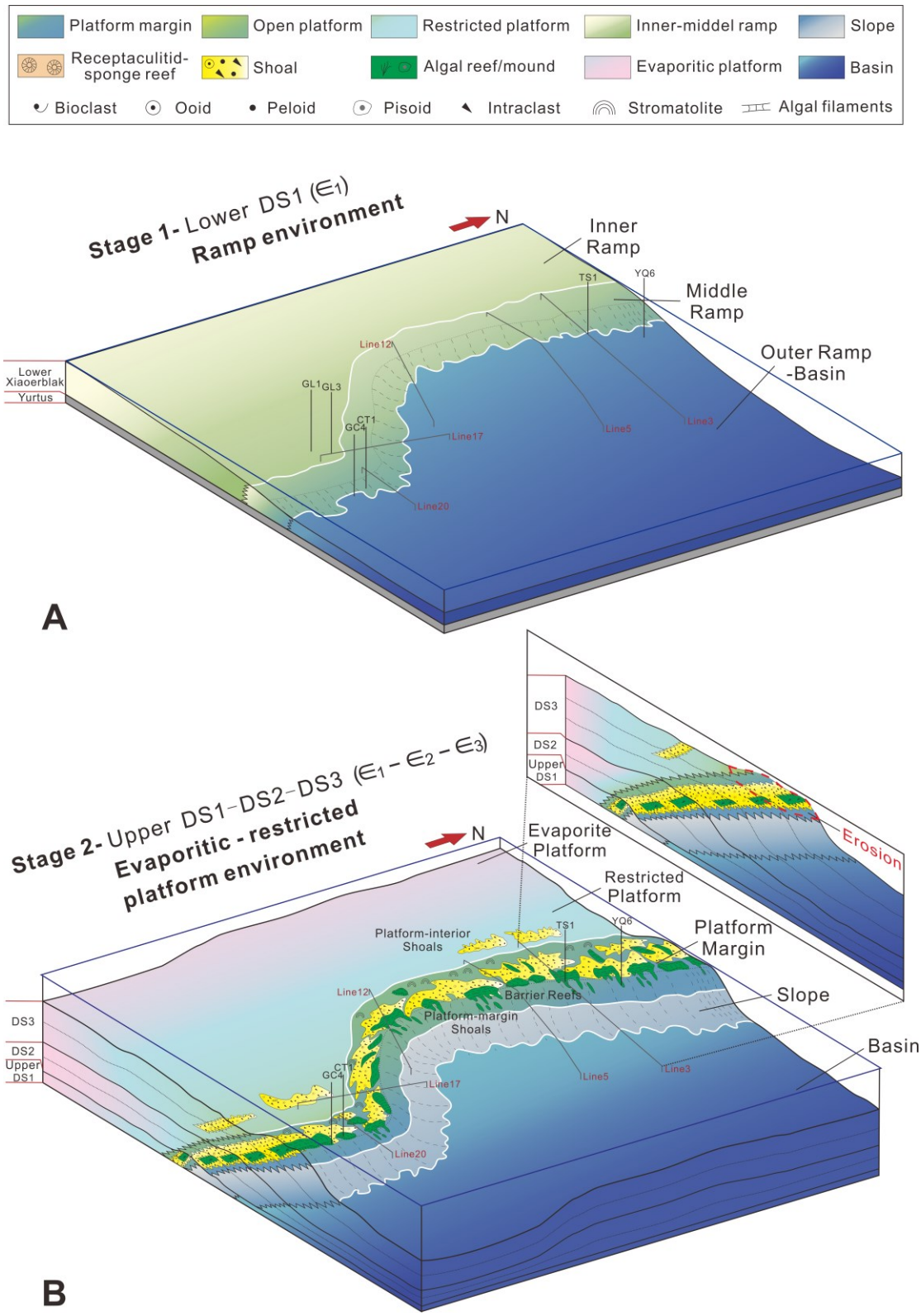

Fig. 13. Paleogeographic setting during Stage 1 (A) and Stage 2 (B). (A) Stage 1 is represented by a Lower Cambrian carbonate ramp, covering a fine-grained clayey unit deposited all over study area. (B) Stage 2 (late Early Cambrian to Late Cambrian) records the development of a high-relief carbonate platform prograding basinward, with differences from the northern to the southern area. The end of System 2 is marked by a subaerial exposure of

the platform top.

Stage 3 (DS4-lower DS5):

During stage 3, the carbonate platform records base level fluctuations that generate diverse stacking patterns (Fig. 12E and Fig. 12F). Creation of accommodation space is limited in the lower part of DS4, as suggested by the progradation of the carbonate platform of about 10 km in the northern and 5 km in the southern platform (Fig. 11H), in absence of a marked aggradation. Carbonate production was likely limited to a narrow zone along the platform margin. Core evidence in southern area indicates that high-amplitude parallel reflections (SF1; Figs. 5 to 9) are low-sedimentation rate micritic limestone in the platform margin (Liu et al., 2017) that record a rapid change in accommodation space and a reduced efficiency of the carbonate factory, resulting in disappearance of algal reef in entire stage 3 (Wang et al., 2011a; He et al., 2017). Due to reduced accommodation, the inner platform area is characterized by restricted to semi-restricted environments (Fig. 14A; Zhao et al., 2014; Chen et al., 2015; Ni et al., 2015) distally bordered by lagoon and barrier shoal mainly containing intraclasts, bioclasts, ooids and algal filaments (Hu et al., 2014). From the upper part of DS4 to lower part of DS5, the situation changes due to increased accommodation in the southern platform, where the platform progrades and aggrades (Fig. 12E), with an increase in the platform-to-basin relief (evaluated in about 1000 m, considering a wave velocity of about ~6000m/s, according to Han et al, 2011, in the Lower Ordovician), along a slope about 20° steep (Fig. 8 and Fig. 9). The effects of the increased accommodation are different in the northern platform, where aggradation and retogradation of the platform margin is observed: here, both platform-to-basin relief and slope angle are reduced, suggesting that carbonate production was not able to overpass the rate of creation of accommodation space (Fig. 12F).

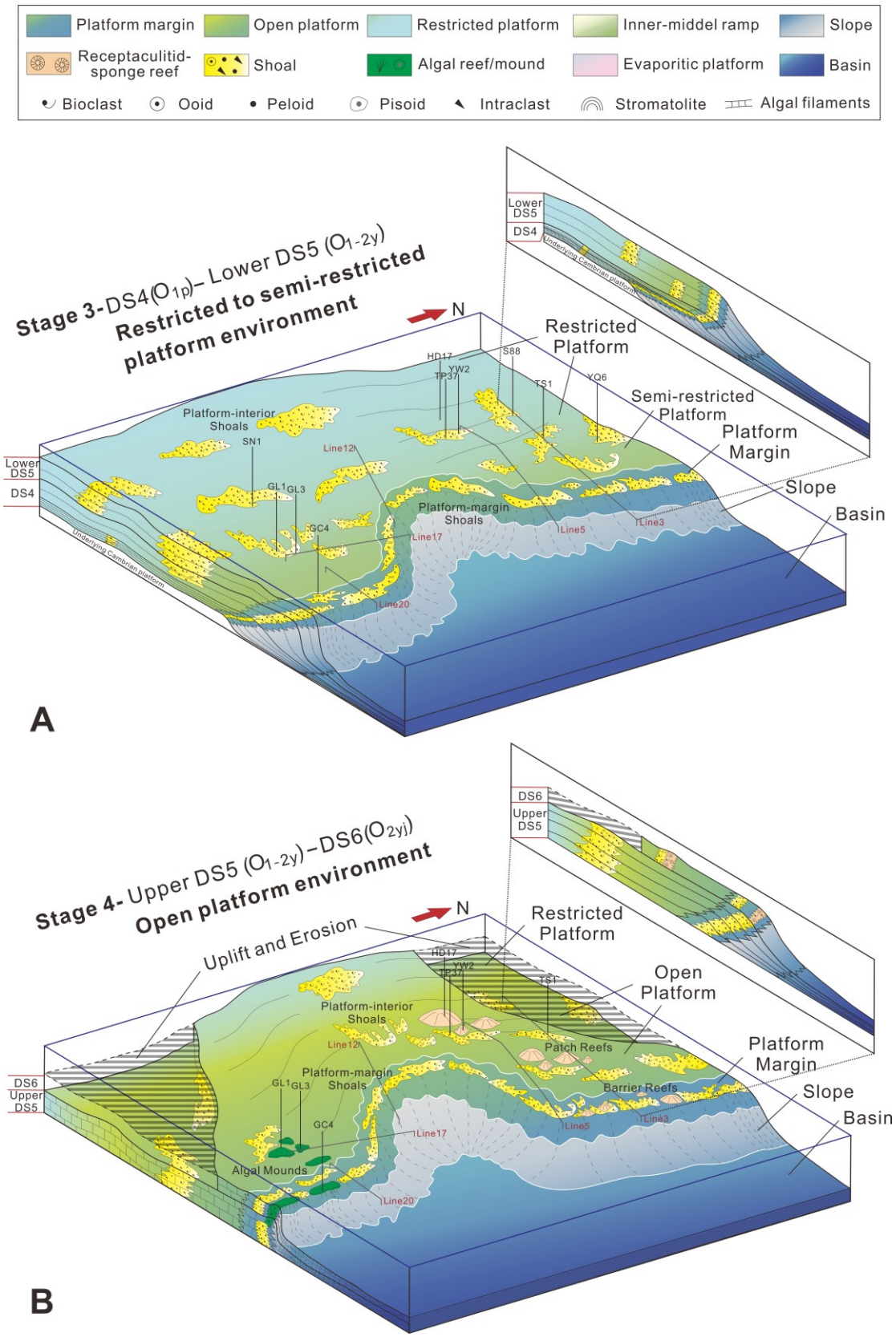

Fig. 14. Paleogeography of the carbonate systems during the Ordovician in study area in stage 3 and stage 4. (A) paleogeography during stage 3, recording different interplay between rate of creation of accommodation space and carbonate production controlling different architecture in the southern and northern platforms during the Early Ordovician. (B)

Paleogeography during stage 4, marked by the subaerial exposure of receptaculitid-sponge reefs in the Middle Ordovician and local erosion caused by tectonic uplift.

Stage 4 (upper DS5 to DS6):

Stage 4 (upper DS5 to DS6) is characterized by a base level rise followed by a fall. Well data (e.g. TP37, LN14, GL1, GC4 and SN501) and outcrops indicate during this stage the dominance of an open platform depositional system (Fig. 12G, 12H and 14B; Gu et al., 2009; Zhao et al., 2014), characterized by shoal facies consisting of grainstone dominated by ooids, bioclasts and intraclasts (Fig. 3F). The reduced thickness of DS6 prevents a detailed interpretation of its internal architectures. As the top boundary (T_7^4) is similar to the top boundary of DS5 (T_7^5) (Figs. 5 to 9), the architecture of platform in DS6 likely resembles that of upper DS5, suggesting a homogeneous patterns throughout stage 4 (Fig. 12G and 12H).

During stage 4, the northern platform shows a progradational and aggradational trend: core data from wells in platform-interior (HD17, LN14) document grainstone or boundstone dominated by receptaculitids, sponges and algae (Zhao, 2014), which indicate the presence of patch reefs in an oolitic-bioclastic shoal. Platform-margin receptaculitids-sponge or calathium reef were clearly verified in outcrop (Liu et al., 2003; Gu et al., 2005, 2009) (Fig. 3J). Hence, despite no wells penetrate DS6 in margin position (as deduced from the seismic interpretation) it is possible to suppose the presence of marginal reefs at the shelf break, bordering a low-angle slope (Fig. 12H). Differently, the southern platform (Fig. 12G) is characterized by an aggradational trend, with a steep slope passing to a deep basin. Well data (e.g., GL1, GL3, GC4) document the occurrence of boundstone dominated by *Nephrocytium*, *Girvanella* and *Epiphyton* (Fig. 3G; Wang et al., 2011b; Fig. 14B).

5.2 Controlling factors on architecture and evolution

The architecture of carbonate platform is determined by the efficiency of the carbonate factory and by the rate of creation of accommodation space, which reflect the interplay of different factors (Scholle et al., 1983; Insalaco et al., 2000; Pedley and Carannante, 2006), including tectonics (Burchette 1988; Watney et al., 2008; George et al., 2009), eustasy (Tucker and Wright, 1990; Pomar and Kendall, 2008; Bergman et al., 2010), hydrodynamics (Bergman et al., 2010), nutrients supply (Lukasik and Simo, 2008), water temperature, paleoceanography and paleoclimate (Shahzad et al., 2018). The studied succession of Early Paleozoic carbonate systems, according to the

seismic profiles, was not affected by significant syndepositional tectonics: tectonics activity is observed during Middle Ordovician, due to block collision at the end of Early Ordovician (Zhang et al., 2007) which caused deformation while limestone with thickness of <100m were deposited (Zhang et al., 2015). The absence of a major tectonic control (stable craton conditions existed during the Cambrian to Early Ordovician; Gao et al., 2016) indicates that the evolution of the carbonate systems was mainly controlled by wide scale base level changes, types and efficiency of carbonate production and inherited topography.

Base level changes significantly control the accommodation space and influence the efficiency of carbonate production, which determine the geometry and internal architecture of carbonate systems (Kendall and Schlager, 1981; Schlager, 2005; Merino Tomé et al., 2012). During the stage 2, the carbonate platforms of the northern and the southern area both document a major continuous progradation (Fig. 12C and Fig.12D), documenting that carbonate production was higher than the rate of creation of accommodation space. Limited extensional tectonics may have favored a large-scale subsidence in the eastern part of the study area (Liu et al., 2016). Observed changes in architecture from end of stage 2 to stage 3 may be related also to local differences in subsidence, as no evident changes of the carbonate factory (type and efficiency) are clearly documented. Other controlling factors may be represented by inherited topography from the previous stages (such as platform to basin relief) or to currents and winds (e.g.; differences from more leeward to more windward conditions). The existence of a steep slope probably controlled the different architecture of the two margins during stage 4, when progradation is observed in the northern platform (characterized by a shallower basinal area and a low-angle slope) but retrogradation characterizes the southern platform. This general architecture was likely controlled also by relative sea-level changes (Zhang, 2017; Yan et al., 2017).

Some of the surfaces separating the different carbonate systems are related to subaerial exposure of the platform, followed by a renewed creation of accommodation space. Other surfaces mark architectural changes likely related to changes in the rate of carbonate production, which is known to be affected by climate, that control temperature and water chemistry (Brachert et al., 1996; Webster et al., 2004; Pomar et al., 2004, 2012) and by the efficiency of the carbonate-producing biota.

The melting of the ice caps at the base of the Cambrian (Berner 1990; Brasier 1992; Runkel et al., 2010; Hearing et al., 2018) caused a global sea level rise, with the

deposition of black shale (with a TOC ranging in the Tarim Basin from 2 to 16%; Zhu et al., 2016; thus representing and important source rock) at a global scale (Banerjee et al., 1997). During transgression, a ramp system developed above the black shales, rapidly evolving to a rimmed carbonate platform before the end of the Cambrian. During the middle Cambrian, at a latitude of some 20°S (Li et al, 2015; Wang et al., 2017), arid conditions characterize the Tarim Block (Steuber and Veizer, 2002; Zhang et al., 2014), as documented by the occurrence of dolomite associated with evaporites in the inner platform domain. During the Ordovician, Tarim Block was characterized by more humid climate, which probably reduced the efficiency of the dolomitizing processes (Zhang et al., 2014).

From the Ordovician, differences in architecture of the carbonate platforms are observed from the southern to the northern area (Fig, 12, 13 and 14). A gradual increase of subsidence from north to south can be invoked to explain the different platform-to-basin relief and slope angle possibly due to the diverse distribution of depth-dependent production rates (Kendall and Schlager, 1981; Schlager, 1981; Bosscher and Schlager, 1992; Burchette and Wright,1992; Pomar and Kendall, 2008), diverse transport rate (wind or current speed; Wright and Burgess, 2005; Williams et al., 2011) and dominance of diverse types of carbonate-producing biota (Pomar, 2001; Pomar and Hallock, 2008). With time, evolution further controlled (Great Ordovician Biodiversification Event, associated with the appearance of new taxa modifying the Cambrian algae-dominated microbial reefs mostly represented by stromatolites or thrombolites) the nature of carbonate producing-biota and the types of skeletal grains produced. During the Middle Ordovician (Yijianfang Formation), cores in the north platform show microbe-receptaculitid-sponge reefs, whereas in the southern platform core facies are represented by microbial mounds only. These observations indicate major differences in reef biota, that can be related to paleoceanographic conditions, currents and wind direction.

6. Conclusion

Interpretation of 2D seismic profiles, constrained by well data and geometric evidence from retrodeformed seismic profiles (restored removing post-depositional deformations) flattened along an originally horizontal stratigraphic surface, supports new architectural and facies distribution models of the Early Cambrian-Middle Ordovician carbonate succession of the east-central Tarim Basin.

The reconstruction of the depositional profile obtained removing the post-depositional deformation identifies four evolutionary stages, from a homoclinal ramp system (Early Cambrian) to overlying flat-topped rimmed systems (Middle Cambrian to Middle Ordovician). The four evolutionary stages are defined by the presence of major surfaces (mostly subaerial exposures) that reflect changes in the rate of creation of accommodation space associated with changes in the carbonate production. In this general evolutionary trend, it was possible to identify a northern and a southern domain, with differences in the platform-to-basin relief, slope angle and depositional architecture. The different evolution of the northern and southern domains reflects different subsidence rates along the platform and changes in the carbonate production/deposition in the two areas, possibly controlled by wind directions, that led to differences in the progradation rate.

The demise of the Cambrian to Middle Ordovician carbonate systems appears to be related to a tectonic event, responsible for the tilting of the succession toward the east (more evident in the northern part of the study area), associated with an uplift (interpreted as a bulge) to the west, where the inner platform of the middle Ordovician were partly eroded.

The interpretation of the seismic facies in the retrodeformed seismic profiles (flattened along the top of the Early Cambrian black shale) produces a new paleogeographic distribution of the facies, suggesting a different position of the platform edge in the different evolutionary stages, which is identified more to the east with respect to what has been proposed earlier. The approach proposed in this study stresses the importance of the crosscheck between geometry of seismic surfaces and seismic facies interpretation: this procedure may be applied to different geological setting, contributing to the development of interpretations when, once identified, the effects of post-depositional deformations are removed, eventually improving the geological knowledge of subsurface successions.

Acknowledgements

This study was financially supported by the Strategic Priority Research Program of the Chinese Academy of Sciences (Grant XDA14010201-02) and the grants from Northwest Exploration and Production Company of SINOPEC (Grant P15030). Petroleum Experts Ltd is acknowledged for the Educational Institution License Agreement for the use of MOVE™ at the University of Milan. Thanks to Prof. Zhiqian Gao (China University of Geosciences, Beijing), Xiangjie Meng and Jing Luo

for their earlier work and valuable suggestions on seismic interpretations. We would also like to thank Eusebio Stucchi (University of Pisa) for the fruitful discussion about the seismic data. We highly appreciate careful and thoughtful reviews by Editor and two reviewers to improve this paper.

References

Bai, Y., Luo, P., Wang, S., Zhou, C.M., Zhai, X.F., Wang, S., Yang, Z.Y., 2017a. Structure characteristics and major controlling factors of Early Cambrian platform margin microbial reef reservoirs: a case study of Xiaoerbulak Formation, Lower Cambrian, Aksu area, Tarim Basin, NW China. Petroleum Exploration and Development. 44(3): 377-386.

Bai, Y., Luo, P., Zhou, C.M., Zhai, X.F., Wang, S., Yang, Z.Y., Wang, S., 2017b. Sequence division and platform sedimentary evolution model of the Lower Cambrian Xiaoerbulak Formation in the NW Tarim Basin. Oil and Gas Geology. 38(1): 152-164 (in Chinese with English abstract).

Banerjee, D.M., Schidlowski, M., Sieber, F., Brasier, M.D., 1997. Geochemical changes across the Proterozoic–Cambrian transition in the Durmala phosphorite mine section, Mussoorie Hills, Garhwal Himalaya, India. Palaeogeography, Palaeoclimatology, Palaeoecology. 132(1-4): 183-194.

Bergman, K.L., Westphal, H., Janson, X., Poiriez, A., Eberli, G.P., 2010, Controlling parameters on facies geometries of the Bahamas, an isolated carbonate platform environment, in Carbonate depositional systems: assessing dimensions and controlling parameters: Springer, Dordrecht, 5-80.

Berner, R.A., 1990, Atmospheric carbon-dioxide levels over Phanerozoic time: Science. 249: 1382-1386.

Bosscher, H., Schlager, W., 1992, Computer simulations of reef growth. Sedimentology. 39: 503-512.

Brachert, T.C., Betzler, C., Braga, J.C., Martin, J.M., 1996. Record of climatic change in neritic carbonates: turnover in biogenic associations and depositional modes (Late Miocene, southern Spain). Geologische Rundschau. 85(2):327-337.

Brasier, M.D., 1992. Global ocean-atmosphere change across the Precambrian-Cambrian transition. Geological Magazine. 129(2): 161-168.

Burchette, T.P., 1988. Tectonic control on carbonate platform facies distribution and sequence development: Miocene, Gulf of Suez. Sedimentary Geology. 59(3-4):179-204.

Burchette, T.P., Wright, V.P., 1992, Carbonate ramp depositional systems. Sedimentary Geology. 79(1-4): 3-57.

Chen, H.H., Wu, Y., Zhu, H.T., Lu, Z.Y., Cao, Z.C., Yun, L., 2016. Eogenetic karstification and reservoir formation model of the Middle-Lower Ordovician in the northeast slope of Tazhong uplift, Tarim Basin. Acta Petrolei Sinica, 37(10): 1231-1246 (in Chinese with English abstract).

Chen, X.J., Cai, X.Y., Ji, Y.L., Zhou, Z.M., 2007. Relationship between large scale unconformity surface and weathering crust karst of Ordovician in Tazhong. Journal of Tongji University (Natural science). 35(8): 1122-1127 (in Chinese with English abstract).

Chen, Y.Q., Yan, W., Han, C.W., Yang, P.F., Li, Z., 2015. Redefinition on structural paleogeography and lithofacies paleogeography framework from Cambrian to Early Ordovician in the Tarim Basin: A new approach based on seismic stratigraphy evidence. Natural Gas Geoscience. 26(10): 1831-1843 (in Chinese with English abstract).

Fan, T.L., Gao, Z.Q., Liu, C., Zeng, Q.B., 2008. The characteristics of Palaeozoic slopes with different geneses and oil/gas plays in the Tarim basin. Earth Science Frontiers. 15(2): 127-136 (in Chinese with English abstract).

Fan, T.L., Yu, B.S., Gao, Z.Q., 2007., Characteristics of carbonate sequence stratigraphy and its control on oil-gas in Tarim Basin. Geoscience. 21(1): 57-65 (in Chinese with English abstract).

Feng, Z.Z., Bao, Z.D., Wu, M.B., Jin, Z.K., Shi, X.Z., Luo, A.R., 2007. Lithofacies palaeogeography of the Ordovician in Tarim area. Journal of Palaeogeography. 9, 447–460 (in Chinese with English abstract).

Fu, H., Han, J.H., Meng, W.B., Feng, M.S., Hao, L., Gao, Y.F., Guan, Y.S., 2017. Forming mechanism of the Ordovician karst carbonate reservoirs on the northern slope of Central Tarim Basin. Natural Gas Industry, B. 4(4), 294-304.

Gao, H.H., He, D.F., Tong, X.G., Wen, Z.X., Wang, Z.M., He, J.Y., 2016. Tectonic-depositional environment and proto-type basins during the depositional period of Middle Ordovician Yijianfang Formation in Tarim Basin. Journal of Palaeogeography. 18(6): 986-1001 (in Chinese with English abstract).

Gao, Z.Q., Fan, T.L., 2015. Carbonate platform-margin architecture and its influence on Cambrian-Ordovician reef-shoal development, Tarim Basin, NW China. Marine and Petroleum Geology. 68, 291-306.

Gao, Z.Q., Fan, T.L., Jiao, Z.F., Li, Y., 2006. The structural types and depositional

characteristics of carbonate platform in the Cambrian-Ordovician of Tarim basin. Acta Sedimentologica Sinica. 2006, 24(1): 19-27 (in Chinese with English abstract).

Gao, Z.Q., Fan, T.L., Yang, W.H., Wang, X., 2012. Structure characteristics and evolution of the Eopaleozoic carbonate platform in Tarim Basin. Journal of Jilin University (Earth Science Edition). 42(3): 657-665 (in Chinese with English abstract).

George, A.D., Chow, N., Trinajstic, K.M., 2009. Syndepositional fault control on lower Frasnian platform evolution, Lennard Shelf, Canning Basin, Australia. Geology. 37(4), 331-334.

Gu, J.Y., Ma, F., Ji, L.D., 2009. Types, characteristics and main controlling factors of carbonate platform. Journal of Palaeogeography. 11(1), 21-27 (in Chinese with English abstract).

Gu, J.Y., Zhang, X.Y., Luo, P., Luo, Z., Fang, H., 2005. Development characteristics of organic reef-bank complex on Ordovician carbonate platform margin in Tarim Basin. Oil and Gas Geology. 26(3): 277-283 (in Chinese with English abstract).

Han, J.F., Zhou, J.M., Jiang, B., Jiang, L.H., Yu, H.F., Hu, Y.F., Yuan, J.Y., Shang, Z.G., 2011. Prediction of carbonate fractured-vuggy reservoir and hydrocarbon accumulation pattern of Yingshan Formation of Lower Ordovician in north slope of Tazhong area, Tarim Basin. Xinjiang Petroleum Geology. 32(3): 281-284 (in Chinese with English abstract).

He, B.Z., Jiao, C.L., Xu, Z.Q., Cai, Z.H., Liu, S.L., Zhang, J.X., Li, H.B., Zhang, M., 2015. Distribution and migration of the Phanerozoic palaeo-uplifts in the Tarim Basin, NW China. Earth Science Frontiers. 22(3): 277-289.

He, D.F., Zhou, X.Y., Yang, H.J., Guan, S.W., Zhang, C.J., 2008. Formation mechanism and tectonic types of intracratonic paleo-uplifts in the Tarim Basin. Earth Science Frontiers. 15(2): 207-221 (in Chinese with English abstract).

He, F., Lin, C.S., Liu, J.Y., Zhang, Z.L., Zhang, J.L., Yan, B., Qu, T.L., 2017. Migration of the Cambrian and Middle-Lower Ordovician carbonate platform margin and its relation to relative sea level changes in southeastern Tarim Basin. Oil and Gas Geology. 38(4):711-721 (in Chinese with English abstract).

Hearing, T.W., Harvey, T.H.P., Williams, M., Leng, M.J., Lamb, A.L., Wilby, P.R., Gabbott, S.E., Pohl, A., Donnadieu, Y., 2018. An early Cambrian greenhouse climate. Science Advances. 4(5): eaar5690.

Hu, X.L., Fan, T.L., Gao, Z.Q., Li, B., Chen, X.Z., Li, Z., Meng, X.J., Li, Z.F., 2014.

Depositional Combination Characteristics and Distribution of Ordovician Carbonate Shoals in the Tarim Basin. Acta Sedimentologica Sinica. 32(3): 418-428 (in Chinese with English abstract).

Insalaco, E., Skelton, P.W., Palmer, T.J., 2000. Carbonate platform systems: components and interactions - An introduction. Geological Society London Special Publications. 178(1):1-8.

Jia, C.Z., 1997. Tectonic characteristics and petroleum in Tarim basin of China; Petroleum Industry Press, Beijing. 115p (in Chinese).

Jiang, H.J., Chen, Q.L., Qiao, G.L., Cao, Z.C., Chu, C.L., 2017. Characteristics and distribution of Lower-Middle Ordovician grain bank in mid-eastern Tarim Basin. Lithologic Reservoirs. 29(5): 67-75 (in Chinese with English abstract).

Kendall, C.G., Schlager, W., 1981. Carbonates and relative changes in sea-level. Marine Geology. 44, 181-212.

Li, J. H., Zhou, X. B., Li, W. B., Wang, H. H., Liu, Z. L., Zhang, H. T., Ta, S. K., 2015. Preliminary reconstruction of tectonic paleogeography of Tarim Basin and its adjacent areas from Cambrian to Triassic, NW China. Geological Review. 61, 1225-1234 (in Chinese with English abstract).

Lin, C.S., Li, H., Liu, J.Y., 2012. Major unconformities, tectonostratigraphic frameword, and evolution of the superimposed Tarim basin, Northwest China. Journal of Earth Science. 23(4): 395-407.

Lin, C.S., Li, S.T., Liu, J.Y., Qian, Y.X., Luo, H., Chen, J.Q., Peng, L., Rui, Z.F., 2011. Tectonic framework and paleogeographic evolution of the Tarim basin during the Paleozoic major evolutionary stages. Acta Petrologica Sinica. 27, 210-218 (in Chinese with English abstract).

Liu, B.L., Rigby, J.K., Zhu, Z.D., 2003. Middle Ordovician lithistid sponges from the Bachu-Kalpin area, Xinjiang, northwestern China. Journal of Paleontology. 77(3): 430-441.

Liu, C., Zhang, Y.J., Li, H.H., Cao, Y.H., Zhao, Y.M., Yang, M., Zhou, B., 2017. Sequence stratigraphy classification and its geologic implications of Ordovician Yingshan formation in Gucheng area, Tarim basin. Journal of Northeast Petroleum University. 41(1): 82-96 (in Chinese with English abstract).

Liu, C.G., Li, G.R., Luo, P., Wang, M., Luo, M.X., Liu, Y.L., 2016. Seismic sequences, evolution and control factors of large Cambrian progradational platform-slope system in the northern Tarim Basin, northwest China. Acta Geologica Sinica. 90(4): 669-687.

Liu, Y.T., Fu, H., Chen, J., Fang, X.L., Huang, C., Jia, W., 2010. Sequence stratigraphy of Cambrian in Bachu-Tazhong area, Tarim Basin. Lithologic Reservoirs. 22(2): 48-53 (in Chinese with English abstract).

Lukasik, J., Simo, J.A., 2008. Controls on Development of Phanerozoic Carbonate Platforms and Reefs—Introduction and Synthesis. (Eds.), Controls on Carbonate Platform and Reef Development. SEPM Special Publication. 89 :5-12.

Merino Tomé, O., Della Porta, G., Kenter, J. A. M., Verwer, K., Harris, P. M., Adams, E. W., Playton, T., Corrochano, D., 2012, Sequence development in an isolated carbonate platform (Lower Jurassic, Djebel Bou Dahar, High Atlas, Morocco): influence of tectonics, eustacy and carbonate production: Sedimentology. 59, 118-155.

Mitchum, R.M., Vail, P.R., Sangree, J.B., 1977. Seismic stratigraphy and global changes of sea-level, part 6: stratigraphic interpretation of seismic reflection patterns in depositional sequences. In: Payton, C.E. (Ed.), Seismic Stratigraphy - Applications to Hydrocarbon Exploration, AAPG Memoir, vol. 26, pp. 117-133.

Neng, Y., W, G.H., Huang, S.Y., Zhang, X., Cao, S.J., 2016. Formation stage and controlling factors of the paleo-uplifts in the Tarim Basin: A further discussion. Natural Gas Industry. 36 (4): 27-34 (in Chinese with English abstract).

Ni, X.F., Shen, A.J., Chen, Y.Q., Guan, B.Z., Yu, G., Yan, W., Xiong, R., Li, W.L., Huang, L.L., 2015. Cambrian carbonate platform types, platform margin segmentation characteristics and exploration enlightenment in Tarim Basin. Natural Gas Geoscience. 26 (7): 1245-1255 (in Chinese with English abstract).

Paumard, V., Zuckmeyer, E., Boichard, R., Jorry, S.J., Bourget, J., Borgomano, J., Maurin, T., Ferry, J., 2017. Evolution of Late Oligocene - Early Miocene attached and isolated carbonate platforms in a volcanic ridge context (Maldives type), Yadana field, offshore Myanmar. Marine and Petroleum Geology. 81:361-387.

Pedley, H.M., Carannante, G., 2006. Cool-water carbonates: depositional systems and palaeoenvironmental controls. Geological Society, London, Special Publications. 255(1):1-9.

Pomar, L., 2001. Types of carbonate platforms: a genetic approach. Basin Research. 13, 313-334

Pomar, L., Bassant, P., Brandano, M., Ruchonnet, C., Janson, X., 2012. Impact of carbonate producing biota on platform architecture: insights from Miocene examples of the Mediterranean region. Earth-Science Reviews. 113, 186-211.

Pomar, L., Brandano, M., Westphal, H., 2004. Environmental factors influencing skeletal grain sediment associations: a critical review of Miocene examples from the western Mediterranean. Sedimentology. 51, 627-651.

Pomar, L., Hallock, P., 2008. Carbonate factories: A conundrum in sedimentary geology. Earth-Science Reviews. 87(3):134-169.

Pomar, L., Kendall, C.G.S.C., 2008. Architecture of carbonate platforms: a response to hydrodynamics and evolving ecology. In: Lukasik, J., Simo, J.A. (Eds.), Controls on Carbonate Platform and Reef Development, SEPM Special Publication. 89, 187-216.

Runkel, A.C., Mackey, T.J., Cowan, C.A., Fox, D.L., 2010. Tropical shoreline ice in the late Cambrian: Implications for Earth's climate between the Cambrian Explosion and the Great Ordovician Biodiversification Event. GSA Today. 2010, 20(11): 4-10.

Schlager, W., 1981. The paradox of drowned reefs and carbonate platforms. Geological Society of America Bulletin. 92: 197-211.

Schlager, W., 2005. Carbonate sedimentology and sequence stratigraphy. SEPM Concepts Sedimentology Paleontology 8.

Scholle, P.A, Bebout, D.G, Moore, C.H., 1983. Carbonate depositional environments. AAPG Mem. 33: 1-708.

Shahzad, K., Betzler, C., Ahmed, N., Qayyum, F., Spezzaferri, S., Qadir, A., 2018. Growth and demise of a Paleogene isolated carbonate platform of the Offshore Indus Basin, Pakistan: effects of regional and local controlling factors. International Journal of Earth Sciences. 107(2): 481-504.

Steuber, T., Veizer, J., 2002. Phanerozoic record of plate tectonic control of seawater chemistry and carbonate sedimentation. Geology. 30: 1123-1126.

Tang, L.J., 1997. An approach to major tectogenesis of Tarim Basin. Experimental Petroleum Geology. 19(2): 108-114 (in Chinese with English abstract).

Torsvik, T.H., Voo, R.V., 2002. Refining Gondwana and Pangea palaeogeography: estimates of Phanerozoic non-dipole (octupole) fields. Geophysical Journal International. 151, 771-794.

Tucker, M.E., Wright, V.P., 1990. Carbonate Sedimentology. Blackwell Publishing Ltd., Oxford, UK.

Wang, G., Zhang, Y.F., Yang, L.M., Wang, Z.Y., Li, Y., 2011b. Transgressive sequences throughout the Yijianfang Formation (Darriwilian, Middle Ordovician) at well Gucheng 4, Tarim Block, NW China. Acta Micropalaeontologica Sinica.

28(1): 137-144.

Wang, Q., Li, S.Z., Zhao, S.J., Mu, D.L., Guo, R.H., Somerville, I., 2017. Early Paleozoic Tarim Orocline: Insights from paleogeography and tectonic evolution in the Tarim Basin. Geological Journal. 52(S1): 436-448.

Wang, Z.M., Jiang, R.Q., Wu, J.C., Zhang, L.J., Xiao, Z.H., 2011a. Carbonate sequence stratigraphic features of Cambrian-Ordovician, Tarim basin. China Petroleum Exploration. 16(1): 9-14 (in Chinese with English abstract).

Watney, W.L., Franseen, E.K., Byrnes, A.P., Nissen, S.E., 2008. Evaluating structural controls on the formation and properties of Carboniferous carbonate reservoirs in the northern Midcontinent, USA. In: Controls on Carbonate Platform and Reef Development, SEPM Special Publication. 89: 125-145.

Webster, J.M., Wallace, L., Silver, E., Potts, D., Braga, J.C., Renema, W., Riker-Coleman, K., Gallup, C., 2004. Coralgal composition of drowned carbonate platforms in the Huon Gulf, Papua New Guinea; implications for lowstand reef development and drowning. Marine Geology. 204(1): 59-89.

Williams, H.D., Burgess, P.M., Wright, V.P., Della Porta, G., Granjeon, D., 2011. Investigating carbonate platform types: multiple controls and a continuum of geometries. Journal of Sedimentary Research. 81: 18-37.

Wright, V.P., burgess, P.M., 2005, The carbonate factory continuum, facies mosaics and microfacies: an appraisal of some of the key concepts underpinning carbonate sedimentology. Facies. 51(1-4): 17-23.

Wu, G.H., Li, Q.M., Xiao, Z.Y., Li, H.H., Zhang, L.P., Zhang, X.J., 2009. The evolution characteristics of palaeo-uplifts in Tarim Basin and its exploration directions for oil and gas. Geotectonica et Metallogenia. 33(1): 124-130 (in Chinese with English abstract).

Xiao, C.T., Jiang, W.D., Pan, Y.T., 1996. Ordovician organic reefs in the Lunnan Area in Northern Tarim. Regional Geology of China. 4: 330-334 (in Chinese with English abstract).

Xiao, X.C., Tang, Y.Q., Li, J.T., 1990. Discussion on geotectonic evolution of north Xinjiang; In: Xinjiang Geological Science (ed.) Project 305 Xinjiang Geological Science Editor Committee, Geological Publishing House, Beijing, pp. 47–67 (in Chinese with English abstract).

Xu, X.S., Wang, Z.J., Wan, F., Fu, H., 2005. Tecotonic paleogeographic evolution and source rocks of the Early Paleozoic in the Tarim Basin. Earth Science Frontiers. 2005, 12(3): 049-057 (in Chinese with English abstract).

Yan, B., Li, Q., Zhang, H., Tian, X.B., Yang, Z.C., 2017. Migration of Cambrian-Ordovician carbonate platform margin and its relationship with the relative sea-level change in east Tarim Basin. Petroleum Geology and Oilfield Development in Daqing, 36(3): 18-24 (in Chinese with English abstract).

Ye, H.M., Li, X.H., Li Z.X., Zhang, C.L., 2008. Age and origin of high Ba–Sr appinite–granites at the northwestern of the Tibet Plateau: Implications for Early Paleozoic tectonic evolution of the western Kunlun orogenic belt. Gondwana Research. 13(1): 126-138.

Yu, B.S., Chen, J.Q., Lin, C.S., 2001. Cambrian-Ordovician sequence stratigraphy on the northern Tarim platform and its correlation with Yangtze Platform and North China platform. Science in China (Series D). 44(4): 373-384.

Yu, B.S., Ruan, Z., Zhang, G., Pan, Y.L., Lin, C.S., Wang, L.D., 2016. Tectonic evolution of Tarim basin in Cambrian–Ordovician and its implication for reservoir development, NW China. Journal of Earth System Science. 2016, 125(2): 285-300.

Zhang, C.W., 1994. Tectonics and evolution of East Xinjiang and nearby plates. Journal of Chengdu University of Technology. 21(4) 1-10 (in Chinese with English abstract).

Zhang, G.Y., Liu, W., Zhang, L., Yu, B.S., Li, H.H., Zhang, B.M., Wang, L.D., 2015. Cambrian – Ordovician prototypic basin, paleogeography and petroleum of Tarim Craton. Earth Science Frontiers. 22(3): 269-276 (in Chinese with English abstract).

Zhang, G.Y., Zhao, W.Z., Wang, H.J., Li, H.H., Liu, L., 2007. Multicycle tectonic evolution and composite petroleum systems in the Tarim Basin. Oil & Gas Geology. 28(5): 653-663 (in Chinese with English abstract).

Zhang, J., Zhang, B.M., Shan, X.Q., 2014. Controlling effects of paleo-climate and paleo-ocean on formation of carbonate reservoirs. Petroleum Exploration and Development, 41(1): 135-143.

Zhang, J.L., 2017. Carbonate sequence sedimentary evolution and control of sea level: A case study of Ordovician in the Gucheng area, Tarim Basin. Natural Gas Industry. 37(1):46-53 (in Chinese with English abstract).

Zhao, M.S., 2014. The research about differences on type, migration and reservoir of reef flat body in platform edge during the Ordovician in Tarim Basin. Chengdu University of Technology.

Zhao, X.Q., Yang, H.J., Ma, Q., Zhou, C.G., Sun, C.H., Yin, T.J., Cai, Q., Sun, S.Y.,

2014. Sedimentary evolution and platform development models for the Ordovician carbonate rocks in northern Tarim Basin. Sedimentary Geology and Tethyan Geology. 34(2): 36-42(in Chinese with English abstract).

Zhao, Z.J., Luo, J.H., Zhang, Y.B., Wu, X.N., Pan, W.Q., 2011. Lithofacies paleogeography of Cambrian sequences in the Tarim Basin. Acta Petrolei Sinica. 32 (6): 937-948 (in Chinese with English abstract).

Zhao, Z.J., Zhao, Y.B., Pan, M., Wu, X.N., Pan, W.Q., 2010. Cambrian sequence stratigraphic framework in Tarim Basin. Geological Review. 56, 609–620 (in Chinese with English abstract).

Zhou, X.J., Lin, C.S., Liu, J.Y., Chen, Y., Li, S.Z., 2006. Distribution and pattern of major tectonic unconformities in the Tarim Basin and the relationship between gas-oil reservoir and theses unconformities. Xinjiang Oil and Gas. 2(1): 1-4 (in Chinese with English abstract).

Zhu, G.Y., Chen, F.R., Chen, Z.Y., Zhang, Y., Xing, Y., Tao, X.W., Ma, D.B., 2016., Discovery and basic characteristics of the high-quality source rocks of the Cambrian Yuertusi Formation in Tarim Basin. Natural Gas Geoscience, 27(1): 8-21 (in Chinese with English abstract).

Zhu, W.B., Zhang, Z.Y., Shu, L.S., Lu, H.F., Su, J.B., Yang, W., 2008. SHRIMP U-Pb zircon geochronology of Neoproterozoic Korla mafic dykes in the northern Tarim Block, NW china: Implications for the long-lasting breakup process of Rodinia. Journal of the Geological Society. 165: 887-890.